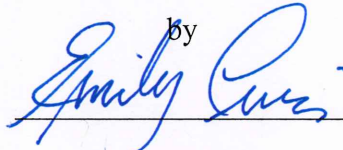


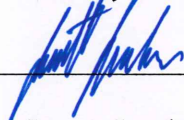
Design and Analysis for the Sphinx-NG CubeSat

A Major Qualifying Project Report
Submitted to the Faculty of the
WORCESTER POLYTECHNIC INSTITUTE
in Partial Fulfillment of the Requirements for the
Degree of Bachelor of Science
in Aerospace Engineering


by



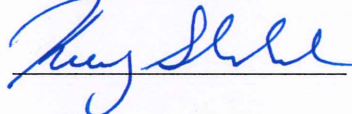
Emily Curci



Jarrett Jacobson



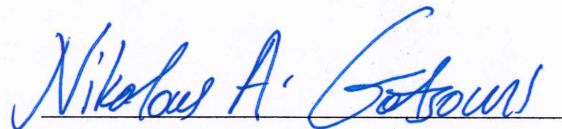
Weston Schlack



Kelley Slabinski

March 24, 2017

Approved by:



Professor Nikolaos A. Gatsonis, Advisor
Aerospace Engineering Program
WPI

Abstract

This project presents the mechanical, orbital, structural design and analysis for a three-unit Cube Satellite (CubeSat) with the SphinX-NG instrument as payload. The goal of the mission is to place the CubeSat on a near-polar, sun-synchronous orbit where it will perform X-ray spectroscopy. The design complies with the Poly-Picosatellite Orbital Deployer (P-POD) and mission requirements. The mechanical design is performed using SolidWorks. Orbital decay analysis using the Systems Tool Kit shows that a 600 km altitude provides a compliant lifetime. Random vibration analysis performed with ANSYS under the maximum expected loads shows compliance. COMSOL analysis of the magnetic fields induced by the onboard magnetic torquers indicates the need for shielding of the onboard magnetometer.

“Certain materials are included under the fair use exemption of the U.S. Copyright Law and have been prepared according to the fair use guidelines and are restricted from further use.”

Acknowledgements

We would like to thank the following individuals and groups for their help and support throughout the entirety of this project.

Project Advisor Professor Nikolaos Gatsonis

ADC Team Professor Michael Demetriou and students Jack Agolli, James Gadoury, and Andrew Rathbun

PTCC&DH Team Professor John Blandino and students Danny Ko, Steve Laudage, Matt Murphy, Daniel Pelgrift, and Sam Young

Table of Authorship

Section	Author
<i>Introduction</i>	EC
<i>Orbital Analysis</i>	JJ
<i>Mechanical Design</i>	KS
<i>Structural Analysis</i>	WS
<i>Analysis of Electromagnetic Interference</i>	WS
<i>Conclusion and Recommendations</i>	EC
<i>Appendix</i>	KS

Table of Contents

Abstract.....	2
Acknowledgements.....	3
Table of Authorship.....	4
Table of Contents.....	5
Table of Figures.....	7
List of Tables.....	8
1 Introduction.....	9
1.1 Overview of CubeSat Missions.....	12
1.2 Review of Previous SphinX-NG CubeSat Designs.....	15
1.3 Systems Engineering Group of the SphinX-NG CubeSat.....	16
1.4 Objectives and Approach.....	16
2 Orbital Analysis.....	18
2.1 CubeSat Deployer Selection.....	18
2.2 Systems Tool Kit.....	19
2.3 Desired Orbit and Launch Site Selection.....	20
2.4 Orbital Lifetime Analysis.....	21
2.5 Integration of CubeSat CAD Model in STK.....	25
3 Mechanical Design.....	26
3.1 P-POD Requirements.....	26
3.2 Sensor, Component, and Instrument Integration.....	31
3.3 Solar Panel Attachment Clips.....	33
3.4 Summary of the Mechanical Design.....	34
4 Structural Analysis.....	36
4.1 Review of Structural Analysis.....	36
4.2 Defeatured SphinX-NG CubeSat Model.....	37
4.3 Analysis Setup in ANSYS.....	38
4.4 Full-Scale Analysis Results.....	39
4.5 Structural Analysis of Circuit Stack.....	44
5 Analysis of Electromagnetic Interference.....	47
5.1 Review of Electromagnetic Interference Analysis.....	47
5.2 Analytical Solution of a Solenoid.....	47
5.3 COMSOL Modeling of a Single Magnetic Torquer.....	49

5.4	COMSOL Modeling of Multiple Magnetic Torquers.....	50
5.5	Discussion of Results.....	51
6	Conclusions and Recommendations.....	53
6.1	Orbital Analysis.....	53
6.2	Mechanical Design.....	54
6.3	Structural Analysis.....	54
6.4	Environmental Analysis.....	54
6.5	Recommendations.....	55
	References.....	56
	Appendix A: List of P-POD Requirements.....	59

Table of Figures

Figure 1: SphinX-NG CubeSat.....	10
Figure 2: SphinX-NG CubeSat Internal View.....	11
Figure 3: Nanosatellites by announced launch years (Kulu, 2017).....	12
Figure 4: Nanosatellites by type (Kulu, 2017).....	13
Figure 5: 3D View of Finalized Orbit.....	24
Figure 6: Orbital Decay Analysis – 500 km.....	24
Figure 7: Orbital Decay Analysis – 600 km.....	25
Figure 8: Pumpkin 3U CubeSat Structure.....	29
Figure 9: Sphinx-NG CubeSat Coordinate System (Billings et al., 2013).....	29
Figure 10: Antenna sits on top of structure, but is still within size constraint.....	30
Figure 11: Sphinx-NG CubeSat Center of Gravity.....	31
Figure 12: SphinX-NG Payload.....	32
Figure 13: Interference between SphinX-NG and Pumpkin Structure (Billings et al., 2013).....	33
Figure 14: Pumpkin Solar Panel Clip.....	33
Figure 15: Custom Solar Panel Clips.....	34
Figure 16: Completed CubeSat Assembly.....	35
Figure 17: Simplified CAD Model in ANSYS.....	38
Figure 18: SphinX-NG CubeSat Modes.....	40
Figure 19: von Mises Stress (X-Axis Vibration).....	40
Figure 20: Deformation (X-Axis Vibration).....	41
Figure 21: von Mises Stress (Y-Axis Vibration).....	41
Figure 22: Deformation (Y-Axis Vibration).....	42
Figure 23: von Mises Stress (Z-Axis Vibration).....	42
Figure 24: Deformation (Z-Axis Vibration).....	43
Figure 25: Simplified Stack CAD Model.....	44
Figure 26: Stack Modes.....	45
Figure 27: Worst Case von Mises Stress.....	45
Figure 28: Worst Case Deformation.....	46
Figure 29: Multi-Slice Plot of a Single Magnetic Torquer.....	49
Figure 30: CAD Model used for COMSOL Simulation.....	50
Figure 31: Magnetic Flux Density on Planes Intersecting at Magnetometer Location.....	51
Figure 32: Magnetic Field Streamlines.....	51

List of Tables

Table 1: Orbital parameters used for initial orbital estimation.....	20
Table 2: Orbital Parameters used for STK Orbital Lifetime Analysis	23
Table 3: Comparison of Orbital Decay for Different Atmospheric Models.....	23
Table 4: List of SphinX-NG CubeSat Components	35
Table 5: Random Vibration loads (Goddard Space Flight Center, 2013)	36
Table 6: Maximum Stress and Deformation.....	43
Table 7: Maximum Stress and Deformation (Stack)	46
Table 8: Magnetic Torquer Parameters	48
Table 9: Comparison of Analytical and COMSOL B Field Intensity for a Single Magnetic Torquer.....	49

1 Introduction

Over the past decade, Cube Satellites (CubeSats) have been increasing in popularity for both educational and commercial missions. The CubeSat concept stemmed from the Space Systems Development Laboratory of Stanford University in 1999 to help meet the educational needs of creating meaningful satellite missions in a quick time frame and for a low cost (CubeSat concept, 2017). A single unit CubeSat, also called 1U, is 10 cm x 10 cm x 10 cm structure with a total mass budget limit of 1 kg. There are variations on this design with 2-unit (2U) and 3-unit (3U), which contain two or three cubes “stacked” together to create the larger structure. The CubeSats were envisioned as platform that can carry “new sensors, communication, and networking capabilities” and provide proof-of-concept for new small-scale space technologies and missions (CubeSat concept, 2017). Stanford University and California Polytechnic State University collaborated on a standardized deployment method for the CubeSats and developed the Poly-Picosatellite Orbital Deployer (P-POD.). P-POD is a tubular design measuring 34 cm x 10 cm x 10 cm, enabling it to hold a standard 3U CubeSat, with some extra space for an antenna. The deployer was designed for integration with multiple kinds of launch vehicles, making it easier for CubeSats to piggyback with a primary payload and be deployed at the correct altitude. This is accomplished due to the fact the CubeSat is loaded into the P-POD in an “off” dormant state as to not interfere with the primary payload. Once deployed, the CubeSat can “activate itself and begin its mission” (CubeSat concept, 2017).

This MQP is a part of a larger conceptual design of a 3U CubeSat, which carries the Solar Photometer in X-rays-Next Generation (Sphinx-NG) instrument. The Space Research Center (SRC) at the Polish Academy of Sciences is leading the design of the Sphinx-NG instrument as a

miniaturized version of the SphinX which flew onboard the Coronas-Photon spacecraft (Sylwester, et al., 2012; Sylwester, L., et al., 2008). WPI has been undergoing the design of the SphinX-NG CubeSat with a series of MQPs reviewed later in this section. The overall goal of the mission is to place the CubeSat into a polar, sun-synchronous orbit at an altitude of 450-650 km so the SphinX-NG can perform solar and extraterrestrial X-ray spectroscopy. The SphinX-NG CubeSat design is shown in Figure 1. An internal view displaying the component layout is shown in Figure 2.

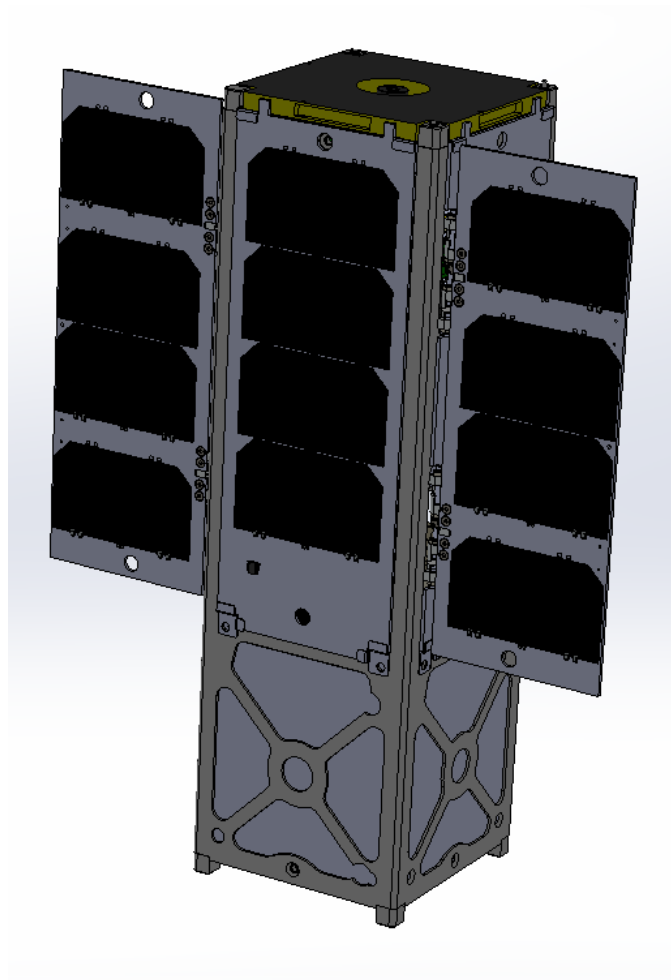


Figure 1: SphinX-NG CubeSat

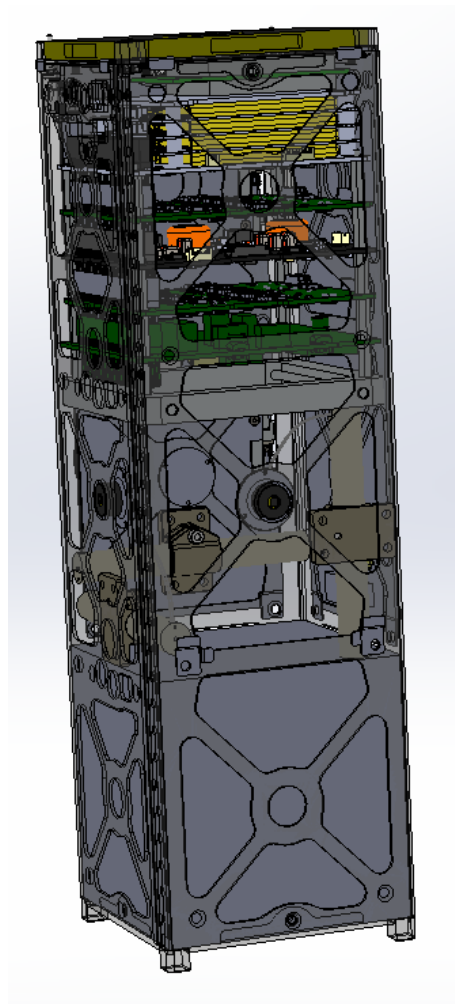


Figure 2: Sphinx-NG CubeSat Internal View

The objectives of this MQP are to perform mechanical design, structural analysis, and orbital analysis for the Sphinx-NG CubeSat in compliance with P-POD requirements, and to conduct electromagnetic interference analysis for the magnetic torquers onboard the CubeSat in compliance with mission requirements.

1.1 Overview of CubeSat Missions

Nanosatellites, or small satellites with a mass of 1-10 kg, have become increasingly popular over the past two decades. CubeSats are a subset of nanosatellites that adhere to the standards set by Stanford University and California Polytechnic State University. To date there have been 483 successfully executed nanosatellite missions, 276 of which have been 3U CubeSats (Swartwout, 2016). Nanosatellites are being developed at an increasing rate, with governments and private companies launching constellations of satellites to collect real time data. In 2017 alone, 600 CubeSat missions are projected to be launched (Kulu, 2017). Figure 3 illustrates the increasing trend of nanosatellite missions.

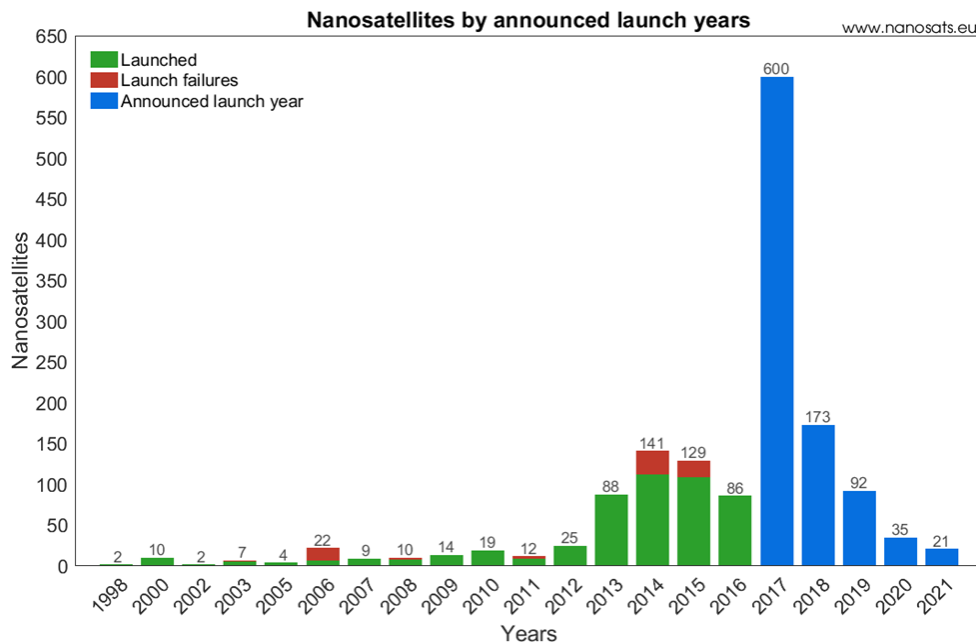


Figure 3: Nanosatellites by announced launch years (Kulu, 2017)

The 3U CubeSat in particular has increased in popularity, as one unit can contain a payload while the other two units house the necessary hardware for other subsystems. Figure 4 shows the increasing popularity of the 3U CubeSat over the all other types (Kulu, 2017).

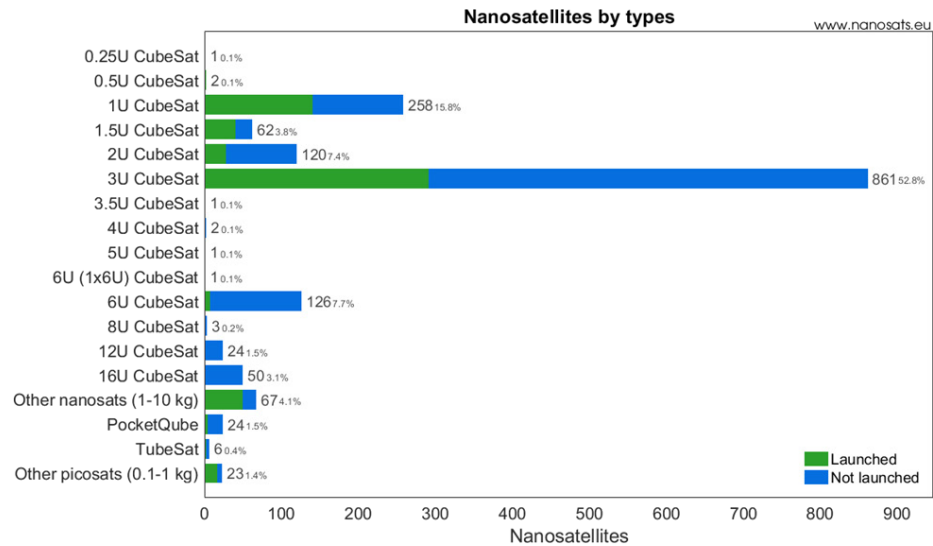


Figure 4: Nanosatellites by type (Kulu, 2017)

Another recent trend is the desire to launch more CubeSats into orbit over the next five years. This is because CubeSat missions cost significantly less than larger satellites. Because of the smaller size, CubeSats can piggyback on another scheduled flight, and can be deployed using the P-POD, or another equivalent deployer. Combined with the lower cost of production and material, a 1U CubeSat would cost around \$52,000 USD (Heyman, 2009). This is compared to approximately \$350 million USD to manufacture and launch a typical communications satellite (Globalcom, 2006).

However, one of the most significant advancements CubeSats have made for space exploration is the introduction of state of the art technology. With easier development and lower costs, CubeSats enable new technologies to be tested and start gaining flight heritage. Advanced concepts have been tested in the fields of communications, optics, synthetic aperture radar, servicing and inspection, power, mission concepts, and propulsion (Kulu, 2017). This focus on technological advancement has been present from the very first CubeSat to the ones currently being developed.

The first truly successful CubeSat (i.e. meeting all the design and size requirements) was the QuakeSat (Swartwout, 2016). The purpose of the satellite was a “proof of concept” mission to detect earthquakes from space (QuakeFinder). The mission launched on June 30, 2003 and used a 3U structure to carry the equipment (QuakeFinder). The CubeSat included a one-foot long magnetometer on an extendable boom, which was used to identify ultra-low frequency (ULF) magnetic signals while in Low Earth Orbit (LEO) (QuakeFinder). This project was sponsored by Stanford University and Lockheed Martin, and not only proved that CubeSats could be cost efficient while providing important scientific data, but also showed the capability of using this as a teaching tool (QuakeFinder). Since QuakeSat, many schools and universities around the world have developed CubeSat programs. Due to their low cost and the availability of off-the-shelf components, it is feasible for students to complete these projects during their academic careers. Since the launch of the first CubeSat, the technological impact has continued to grow. One of the most recent designs is the University of Utah’s 3U CubeSat that houses a telescope and operates at an altitude of 500 km, while providing ground coverage over a 61 km by 4.6 km area (Kulu, 2017). This project showed that more area could be covered from space with significantly lower cost and less complex systems than on prior conventional satellites.

Universities are not the only entities using the CubeSat concept. Private companies are particularly interested in multiple CubeSats that form orbital constellations. For example, Planet Labs has as a goal to “image the entire Earth every day, and make global change visible, accessible, and actionable” (Planet, 2017). They have created the largest constellation of Earth-imaging satellites, which has helped both businesses and humanitarian organizations (Planet, 2017). As this company grows and develops, so does CubeSat technology. There is now a larger market for off-

the shelf CubeSat products (Planet, 2017). With more satellites being developed, there have also been heightened regulations to mitigate space debris. Through the efforts of universities and private companies, CubeSats will continue to increase in popularity and advance the development of spaceflight technology and promote scientific discoveries.

1.2 Review of Previous SphinX-NG CubeSat Designs

During the 2011-12 academic year, WPI began its relationship with the Polish Academy of Sciences in Poland and NASA's Goddard Space Flight Center to develop a 3U CubeSat, which could house the SphinX-NG (Dopart et al., 2012). The 2011-12 group consisted of 16 students divided into three MQP teams. Dopart et al. (NAG-1102, 2012) presents orbital and decay analysis using Systems Tool Kit (STK), the selection of the GPS and the magnetometer, ambient and induced environment analysis using COMSOL, and a preliminary discussion on command and data handling and the on-board computer. Farhead et al. (MAD-D11A, 2012) presents the hardware selection of the gyroscope, sun sensors, and magnetorquers, attitude determination algorithms, and control policies. Bauer et al. (JB3-CBS2, 2012) presents environmental and component-induced thermal analysis, component and assembly design, preliminary stress analysis, and power generation and management.

The most recent version of the CubeSat was developed by sixteen students separated into three groups during the 2012-13 academic year. Billings et al. (NAG-1204, 2013) presents the mechanical design, orbital analysis using STK, and an analysis of electromagnetic interference induced by the magnetorquers. Dawson et al. (MAD-2013, 2013) presents the selection of sensor, actuator, and processor hardware, the attitude control algorithm using MATLAB, and the preliminary design of an attitude control test-bed stand. Hanley et al. (JB3-CBS3, 2013) presents

the analysis of the CubeSat power budget, design of the wiring diagram, thermal analysis using STK and COMSOL, and telecommunications analysis using STK.

1.3 Systems Engineering Group of the Sphinx-NG CubeSat

To continue advancing the Sphinx-NG CubeSat design during the academic year 2016-17, a group of 12 aerospace engineering majors constituted the Systems Engineering Group (SEG). The SEG was split into three separate teams (and MQPs) addressing the various subsystems and mission operations of the CubeSat:

- Mechanical, Structural, Orbital and Environmental (NAG-1701)
- Power, Thermal, Command and Data, Communications, Mission Ops (JB3-1701)
- Attitude Determination and Control (MAD-1701)

Each team carried out its respective tasks independently and presented its progress at a weekly meeting of the SEG. The success of the project depended on how well the teams communicated with one another to share important mission details. To accomplish this, teams also used the SEG meetings to ask other teams for required information or create action items for other teams to complete.

1.4 Objectives and Approach

The Objectives and Approach of this MQP are as follows:

1. Perform Orbital Analysis in compliance with P-POD requirements.
 - a. Identify potential CubeSat deployers using flight history and mission requirements.
 - b. Develop an orbit that could be attainable and still achieve the science requirements for the SphinX-NG instrument using the STK software.
 - c. Complete a lifetime analysis of the CubeSat to ensure it would meet government

and deployer standards for small satellites.

- d. Integrate the CAD model into the STK software to achieve detailed analysis of the satellite in orbit.
2. Perform Mechanical Design in compliance with P-POD requirements.
 - a. Use SolidWorks to revise the CAD files from Billing et al. (2013) with new instruments selected by the other subsystems.
 - b. Ensure that the SphinX-NG CubeSat meets the launch requirements of the selected deployer.
 - c. Finalize the design to be used as a base for structural analysis.
 3. Perform Structural Analysis in compliance with P-POD requirements.
 - a. Develop defeatured models of the SphinX-NG in SolidWorks.
 - b. Use ANSYS to perform a detailed modal and vibration analysis for the SphinX-NG CubeSat structure, including its internal components.
 - c. Perform modal and vibration analysis for the circuit stack.
 - d. Verify that all components and the final assembly adhere to the launch requirements for the deployer.
 4. Environmental Analysis in Compliance with Mission Requirements
 - a. Use analytical models to find the magnetic field produced by the magnetorquers.
 - b. Use COMSOL to obtain a numerical solution for the magnetic field produced by the magnetorquers.
 - c. Determine the effects of the CubeSat structure on induced magnetic fields.
 - d. Ensure that induced magnetic fields do not interfere with the CubeSat instruments.

2 Orbital Analysis

In this chapter, orbital analysis is performed using the Systems Tool Kit (STK) software to determine orbital lifetime in compliance with P-POD requirements. Additionally, orbital modeling allows for mission planning and evaluation of power and design of thermal subsystems.

2.1 CubeSat Deployer Selection

CubeSat deployment is achieved by piggybacking as an auxiliary payload on a rocket launching a larger spacecraft. The two prominent CubeSat deployment services are the NanoRacks CubeSat Deployer (NRCSD) produced by NanoRacks LLC and the Poly Picosatellite Orbital Deployer (P-POD) developed by California Polytechnic State University. The NRCSD is housed on the International Space Station (ISS). CubeSats to be deployed are delivered as cargo on regular missions to the ISS. Achievable orbital parameters are limited by the ISS's orbit: 485-500 km altitude and 51.6° inclination. NRCSD is thus ruled out as a potential deployer, as it is incapable of delivering our CubeSat to the desired inclination of 98.44° .

P-POD is a CubeSat deployer designed for deploying CubeSats as a secondary payload directly from a launch vehicle. This deployer benefits from the flexibility of achieving a wide range of orbits, with the drawback that one must wait until a mission capable of delivering the CubeSat to the desired orbit arises. California Polytechnic State University has published a document outlining the requirements that must be met for CubeSat launching from P-POD. Due to its flexibility and ability to deliver our CubeSat to our desired orbit, we have chosen P-POD as our deployment mechanism.

2.2 Systems Tool Kit

Systems Tool Kit (STK) is a software suite created by Analytical Graphics, Inc. (AGI), offering tools for complex orbital design and analysis. STK operates using several physics based propagators split between three tiers of accuracy: Analytic Propagators (low fidelity), Semi-Analytic Propagators (medium fidelity), and Numerical Integration (high fidelity). Analytic propagators use straightforward approximations to model the motion of an object. These propagators include the TwoBody, J2Perturbation, and J4Perturbation. The TwoBody propagator is the simplest propagator in STK, modeling the Earth and objects as point masses. The J2Perturbation and J4Perturbation propagators account for orbital variations due to Earth's oblateness. These models treat Earth as an oblate sphere, with J2Perturbation only accounting for the first order J2 term (the most dominant term). J4Perturbations considers second order J2 terms and first order J4 terms, resulting in increased accuracy. The J2 and J4 terms cause the RAAN and argument of perigee to drift over time, an effect not modeled by the two-body model. These models do not include an atmospheric drag model (Systems Tool Kit, 2017).

The Semi-Analytic propagators allow for more accurate predictions for orbits by including numerical techniques. These propagators include the effects of solar and lunar gravitation, gravitational resonance, and basic atmospheric drag models. Utilizing numerical techniques increases the complexity and number of calculations, taking more time and computational power to run simulations.

Numerical Integration propagators, such as the High-Precision Orbit Propagator (HPOP), allow for the most accurate orbital predictions. The HPOP model uses no approximations, and instead fully applies numerical algorithms. These calculations are significantly more complex than

the other tiers of propagators and completely sacrifice calculation speed in favor of a high degree of accuracy.

Our analysis is performed using the J2Perturbator, as a higher degree of accuracy is unnecessary for our initial orbital and orbital decay analysis. Orbital decay analysis is modeled using STK's Lifetime Tool. This tool provides an estimate for orbital decay by accounting for atmospheric drag and perturbation effects. AGI recommends using the high-fidelity propagators such as HPOP or Astrogator for accurate analysis and prediction of re-entry location. Our mission does not require analysis of re-entry location, as the SphinX-NG CubeSat will break up due to atmospheric drag.

2.3 Desired Orbit and Launch Site Selection

In Dopart et al. (2012), STK was used to perform an initial investigation to establish an optimal ascending node. Analysis concluded that an ascending node of 06:00:00 provided an orbit with no time spent in eclipse. This was desirable because it maximizes the orbital time that can be spent for solar panel power generation and data collection. In Billings et al. (2013) the orbital analysis was expanded on by establishing additional orbital parameters shown in Table 1.

Table 1: Orbital parameters used for initial orbital estimation

Parameter	Value
Eccentricity	0
Inclination	98.44°
RAAN	142.252°
Argument of Perigee	0°
True Anomaly	0°

The parameters shown in Table 1 were used as a starting point for the orbital decay analysis. The main U.S. launch facilities capable of achieving orbital altitudes are the Kennedy Space

Center, Cape Canaveral Air Force Station, Vandenberg Air Force Base, Kodiak Launch Complex, and the Mid-Atlantic Regional Spaceport. The only facility with a consistent launch schedule that is capable of high inclination polar sun-synchronous orbits is Vandenberg Air Force Base, located in California. This location has the advantage of a large range of launch azimuth angles, making it a flexible location for different achieving a variety of orbits. Typical missions from this facility are polar orbits of 97-98° inclination (Davis, 2012).

A search was performed using STK's database in order to identify launches from the Vandenberg Air Force Base within the last 60 years with orbital parameters similar to the desired orbit. A periapsis and apoapsis altitude of 500-800 km and an inclination of 98-99° were used as search parameters. 188 satellite launches met these criteria, with 22 since 2000. Based on this historical data, it is reasonable to conclude that there will be a launch capable of delivering the SphinX-NG CubeSat to or close to the desired orbit.

2.4 Orbital Lifetime Analysis

P-POD requirement 2.4.5 states that the orbital decay lifetime of the CubeSat must be less than 25 years after the end of its mission life. This constraint is imposed to reduce the accumulation of space debris. Lower altitude orbits have shorter orbital lifetimes due to increased atmospheric drag. STK calculates orbital decay as a function of drag coefficient, drag area, area exposed to sun, mass, atmospheric density model, solar flux, and geomagnetic activity. It was found that the choice of atmospheric model plays a large role in the calculated orbital lifetime. Billings et al. (2013) used the Standard Reference Atmosphere 1977¹ (Jacchia, 1977) in their analysis to allow for a comparison of the results from STK with results from NASA's Debris Assessment Software

¹ Billings et al. (2013) incorrectly referred to the Jacchia 1977 model as the Jacchia 1976 model.

(DAS), which uses the Jacchia 1977 model (NASA, 2012). DAS was not used in this analysis in order to provide the freedom of using different atmospheric density models in STK. To achieve the most accurate estimate of the projected orbital lifetime, the three most widely used models were reviewed. The U.S. 1976 Standard model is widely used in modeling atmospheric properties (NASA, 1976). It was developed using annual averages, but is mathematically derived using many simplifying assumptions. This model was dismissed due to its lack of robustness and inaccuracies as altitude increases. The next model evaluated was the Standard Jacchia Reference Atmosphere 1970 (Jacchia, 1965). The U.S. Navy and Air Force previously used this robust model as the standard for space object orbit analysis. Jacchia 1970 takes into account latitudinal, seasonal, geomagnetic, and solar effects. Additionally, the model incorporates empirical spacecraft drag data. It models altitudes of 90-2500 km and has a statistical accuracy of 15%. The last model evaluated was the NRLMSISE-00, developed by the U.S. Naval Research Laboratory (Picone et al, 2001). This model is regarded as being superior to the Jacchia family of models. The inputs for the model are date, time, geodetic coordinates, altitude, local apparent solar time, 81-day average of F10.7 solar flux, daily F10.7 solar flux for the previous day, and the daily magnetic index. The model outputs the number density of the major atmospheric constituents and temperature. A unique feature of the model is its ability to predict anomalous oxygen number density, which an important contribution to high altitude drag estimation. The model additionally incorporates empirical satellite drag data. Based on this review, it was concluded that the NRLMSISE-00 model is the most robust and accurate model for atmospheric density.

STK allows for a variety of inputs to achieve a more accurate prediction of orbital decay. These inputs include drag coefficient, drag area, area exposed to the Sun, and satellite mass. The

orbital lifetime analysis was performed using the parameters shown in Table 2.

Table 2: Orbital Parameters used for STK Orbital Lifetime Analysis

STK Propagator	J2Perturbation
Solar Flux File	SolFlx_CSSI.dat
Start Date	January 1, 2019
Altitude	500-800 km
Inclination	98.44°
RAAN	142.252°
Argument of Perigee	0°
Ascending Node	06:00:00
Drag Coefficient	2.2
Drag Area	0.055 m ²
Area Exposed to Sun	0.07 m ²
Satellite Mass	4 kg

A comparison of the orbital lifetime predictions for decay at an altitude of 65 km for each of the atmospheric models considered is presented in Table 3.

Table 3: Comparison of Orbital Decay for Different Atmospheric Models

Altitude (km)	U.S. 1976 Standard (years)	Jacchia 1970 Lifetime (years)	NRLMSISE-00 Lifetime (years)
500	2.7	4.8	4.8
600	14.3	17.9	17.8
700	67.4	>>25	>>25
800	328.3	>>25	>>25

Based on the orbital analysis performed in STK, the altitude of 600 km was chosen as a desirable insertion point. At this altitude, the NRLMSISE-00 model predicts that the SphinX-NG CubeSat will have an orbital lifetime of 17.8 years, meeting the P-POD requirement of an orbital lifetime less than 25 years. Figure 5: 3D View of Finalized Orbit Figure 5 shows an STK rendering of the finalized orbit.

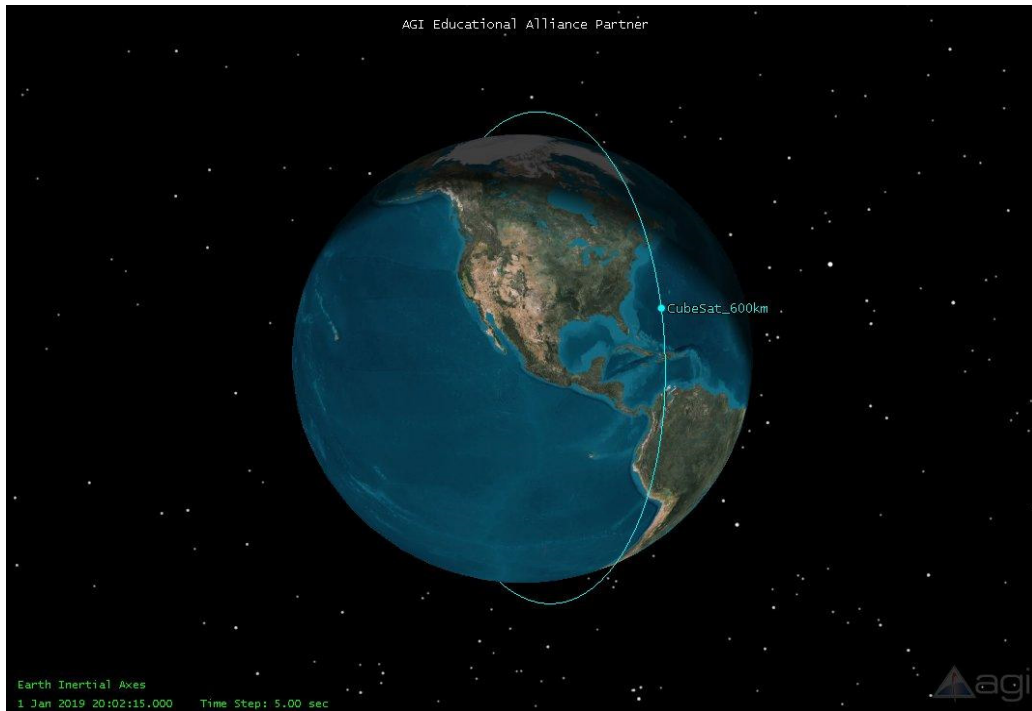


Figure 5: 3D View of Finalized Orbit

Figure 6 and Figure 7 plot the orbital decay of the 500 km and 600 km orbits respectively. The orbital lifetime exhibits a positive feedback decay, with altitude loss rate increasing as altitude decreases. Atmospheric drag effects cause the orbit to shift cyclically from circular to elliptical repeatedly, converging as altitude decreases.

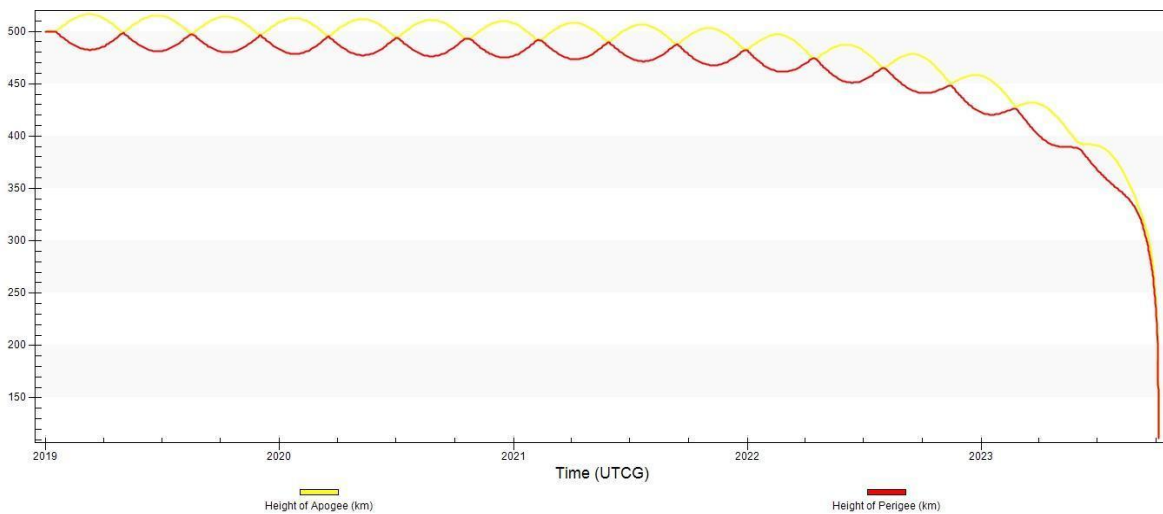


Figure 6: Orbital Decay Analysis – 500 km

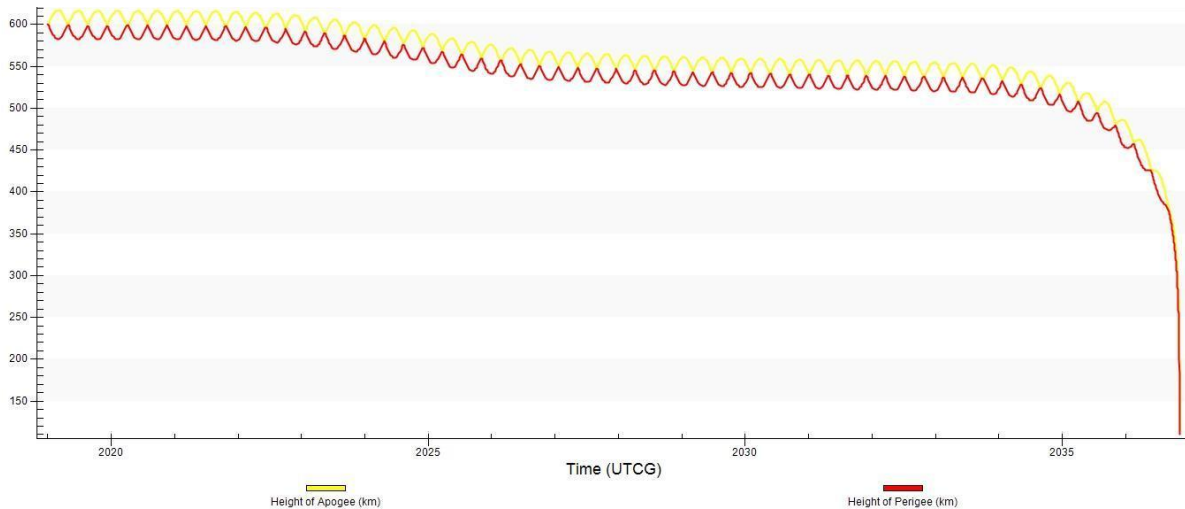


Figure 7: Orbital Decay Analysis – 600 km

2.5 Integration of CubeSat CAD Model in STK

STK features satellite CAD model integration for detailed analysis beyond orbital parameters. Basic attitude control of the CubeSat model for power generation analysis is accomplished using the “Nadir alignment with Sun Constraint” option. This points the CubeSat Z-axis toward Earth while simultaneously attempting to keep the X-axis pointed towards the Sun. Solar panel power generation throughout an orbit can be analyzed by providing STK with the solar panel area and efficiency. STK will then calculate the power generated as a function of time based on position, time, and angle towards the sunlight vector. A similar analysis can be performed to calculate thermal effects. CAD model integration with STK additionally allows analysis and optimization of sensor locations by making sure that the sensors are placed in positions that provide the most favorable lines of sight. A simplified CAD model containing the SphinX-NG CubeSat structure and solar panels was created using SolidWorks and Blender and was imported into STK. The STK file containing this model and the updated orbital parameters was distributed to the other subsystem teams for use in their analysis.

3 Mechanical Design

The design of the SphinX-NG CubeSat has undergone two iterations (NAG-1102, NAG-1204). The first objective of the mechanical design in this project is to use SolidWorks and revise extensively the CAD files from Billing et al. (2013), incorporating new instruments and subsystems. The second objective is to ensure that the SphinX-NG CubeSat meets the launch requirements of the selected deployer. This chapter presents the mechanical design.

3.1 P-POD Requirements

Poly Picosatellite Orbital Deployer (P-POD) is a common deployer of microsatellites, as mentioned in the previous sections of this paper. The P-POD deployers have a set of requirements to meet to be eligible for launch from their particular deployers. A full list of requirements can be found in Appendix A. The requirements that pertain to the structure of the SphinX-NG CubeSat affect the work of this team as well as the work of the other teams, because all sensors and subsystems need to comply within the P-POD requirements. The points that were most pertinent to the structural design of the SphinX-NG CubeSat, in order of appearance on the spreadsheet in Appendix A, were:

1. All parts shall remain attached to the CubeSats during launch, ejection, and operation. No additional space debris shall be created.
2. CubeSat materials shall satisfy the following low out-gassing criterion to prevent contamination of other spacecraft during integration, testing, and launch.
3. Total Mass Loss shall be less than or equal to 1%.
4. The CubeSat shall use the coordinate system such that the -Z face of the CubeSat will be inserted first into the P-Pod.

5. The CubeSat configuration and physical dimensions shall be as shown.
6. CubeSat shall be 100.0 ± 0.1 mm wide.
7. CubeSat shall be 340.5 ± 0.3 mm tall.
8. All components shall not exceed 6.5 mm normal to the surface of the P-POD, other than the designated CubeSat rails.
9. Deployables shall be constrained by the CubeSat. The P-POD rails and walls shall not be used to constrain deployables.
10. Rails shall have a minimum width of 8.5 mm.
11. The rails shall not have a surface roughness greater than 1.6 micrometers.
12. The edges of the rails shall be rounded to a radius of at least 1 mm.
13. The ends of the rails on the +Z face shall have a minimum surface area of 6.5 mm x 6.5 mm contact area for neighboring CubeSat rails.
14. At least 75% of the rails shall be in contact with the P-POD rails. 25% of the rails may be recessed and no part of the rails shall exceed the specification (at least 255.4 mm rail contact).
15. CubeSat shall not exceed 4.0 kg mass.
16. The CubeSat center of gravity shall be located within a sphere of 2 cm from its geometric center.
17. Aluminum 7075 or 6061 shall be used for both the main CubeSat structure and the rails. If other materials are used the developer shall submit a DAR and adhere to the waiver process.
18. The CubeSat rails and standoff, which contact the P-Pod rails and adjacent CubeSat

standoffs, shall be hard anodized aluminum to prevent and cold welding with the P-POD.

19. Subjected to Random Vibration Test to verify its ability to survive the lift-off environment and also to provide a final workmanship vibration test. For small payloads the test is required. The acoustic environment at lift-off is usually the primary source of random vibration, however other sources of random vibration must be considered. Protoflight hardware shall be subjected to a random vibration test to verify flight worthiness and workmanship. The test level shall represent the qualification level (flight limit level plus 3 dB). The test should cover the full 20-2000 Hz frequency range.

Requirements 1-3, 8, 10-14, and 17-18 can be satisfied by using a flight-tested, pre-fabricated structure for the CubeSat. Many companies make specifically CubeSat parts, and these requirements are uniform throughout all deployer types, therefore the companies that make CubeSat parts pre-test and design parts to meet the necessary requirements. The Pumpkin 3U CubeSat structure shown in Figure 8 was selected for the SphinX-NG CubeSat. The main requirements that influenced the design are 4-7, 9, 15, 16, with 19 discussed in Sections 4.3 and 4.4.

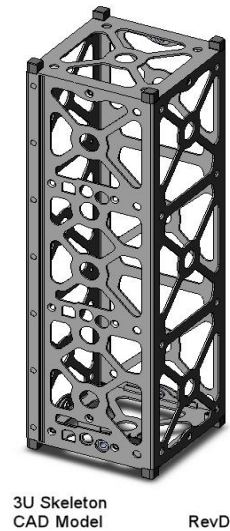


Figure 8: Pumpkin 3U CubeSat Structure

Requirements 4 and 5 are met by determining a coordinate system for the SphinX-NG CubeSat ensuring compliance by all design teams. This coordinate system is shown in Figure 9. Note that the X axis points through the sun-facing side of the CubeSat.

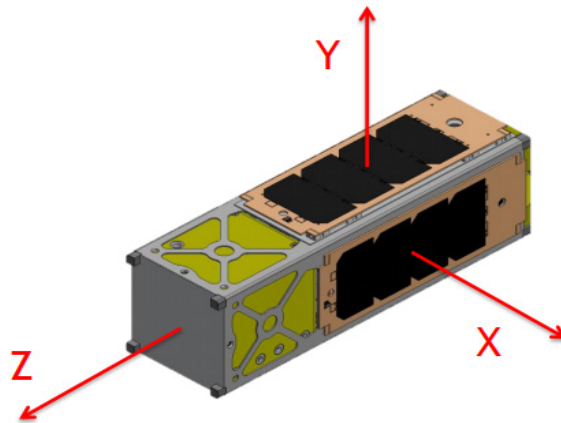


Figure 9: SphinX-NG CubeSat Coordinate System (Billings et al., 2013)

To ensure that requirements 6 and 7 are met, the design did not allow any components to be placed outside the main CubeSat structure aside from the antenna, which attaches at the top, and the solar panels, which attach to the sides. As shown in Figure 10, the top of the CubeSat has an

indent where the main structure ends but the rails extend. This indent is intended for the placement of the ISIS UHF Antenna.

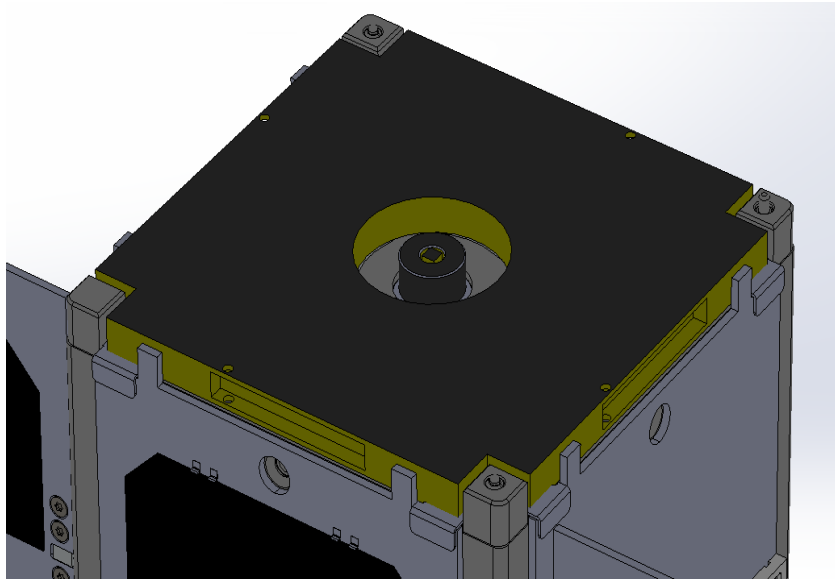


Figure 10: Antenna sits on top of structure, but is still within size constraint

ClydeSpace provides the solar panels chosen by the power group. A 2U body panel is used for the sun-facing side, with two 2U deployable panels on the adjacent sides. Since the panels are designed for CubeSat use, they fall within the width tolerance limits, and are able to fit within the deployer without using the deployer as the means of restraint (thus meeting requirement 9).

Requirements 15 and 16 were used by all three design teams as a guide to use parts that minimize mass, and to place them so that the center of gravity of SphinX-NG CubeSat is located within 2 cm of the geometric center along each axis. The center of gravity is located at (0.4667, 0.1273, 1.7850) cm relative to the geometric center and is shown in Figure 11. This results in a total distance of 1.849 cm away from the geometric center, which is less than the P-POD limit of 2 cm.

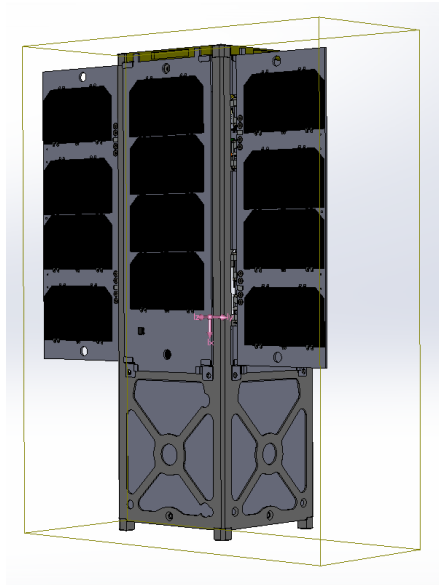


Figure 11: SphinX-NG CubeSat Center of Gravity

The other requirements found in Appendix A were then distributed to the respective groups, so that the SphinX-NG CubeSat would pass all aspects of inspection.

3.2 Sensor, Component, and Instrument Integration

Following the requirements outlined in Appendix A, the design groups MAD-1701 and JB3-1701 proceeded with component selection. To allow for accurate bookkeeping, a table was set up with a list of components, and whether they had changed from the Billings et al. (NAG-1204, 2013). This made it possible to keep track of which parts had changed, and which parts did not need to be updated. A final list of components is shown in Section 3 of this chapter.

The updates on parts followed the following process:

1. The design teams were asked to inform the Mechanical Design of their decisions on parts and components and if possible, obtain an updated CAD file.
2. Once new parts were identified, they were then integrated into the design at the necessary location keeping in mind the P-POD requirement for the center of gravity.

3. Using the new placements of the components, proper mates and relationships were put in place to keep the parts together before the final screws and assemblies were put in.

The new parts integrated in the design include:

ClydeSpace 2U solar panels that are designed to meet P-POD requirements. In Billings et al. (2013), custom hinges were designed to attach the solar panels. However, the newly selected solar panels from ClydeSpace include hinges, which are flight-tested and meet material requirements.

A ClydeSpace USM-1192 battery.

The ClydeSpace CubeSat OBC (On-Board-Computer).

The SphinX-NG shown in Figure 12 was also integrated into the mechanical design. The preliminary CAD available for the SphinX-NG resulted in interference with the rails use to load the 3U CubeSat as shown in Figure 13. All alternative 3U structures examined exhibited the same design issue. To resolve this, a “black box” shell of the recommended dimensions was used as a placeholder for the SphinX-NG and the recommended dimensions were sent to the SphinX-NG design team (Gatsonis, personal communication) for further development.

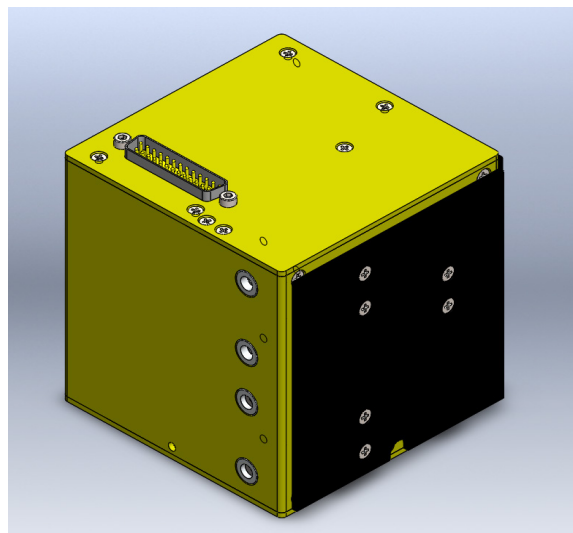


Figure 12: SphinX-NG Payload

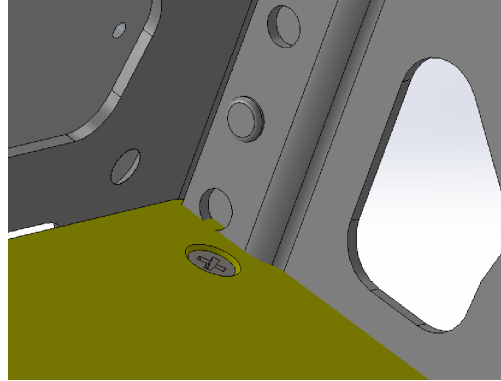


Figure 13: Interference between SphinX-NG and Pumpkin Structure (Billings et al., 2013)

3.3 Solar Panel Attachment Clips

Pumpkin, Inc. provides solar panel clips (shown in Figure 14) which hold the solar panels onto the CubeSat structure. These clips are constructed from sheet aluminum and integrate with the top and bottom of the Pumpkin CubeSat structure. However, these clips are designed to be used when the solar panels are the same size as the structure (i.e. 2U solar panels on a 2U structure). The SphinX-NG CubeSat uses 2U solar panels on a 3U structure, so the Pumpkin clips could not be used to fix the bottom side of the panels to the structure. Custom solar panel clips were designed using the same material as the Pumpkin clips. The custom clips use screw holes in the Pumpkin structure and are shown in Figure 15.

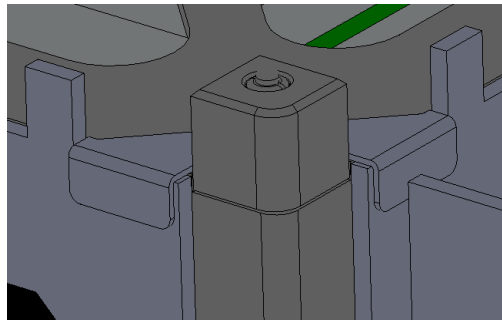


Figure 14: Pumpkin Solar Panel Clip

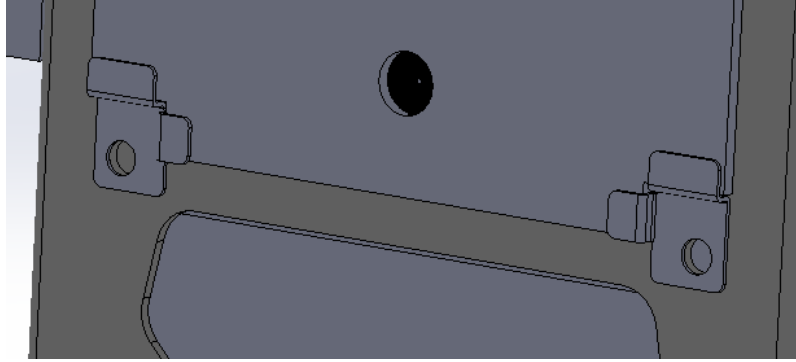


Figure 15: Custom Solar Panel Clips

3.4 Summary of the Mechanical Design

To finalize the mechanical design all the components of the SphinX-NG CubeSat were attached to the main structure with screws that will meet P-POD requirements. These connections keep the parts together, and create a unified structure. One of the main challenges faced in implementing screws was using the SolidWorks interface. If the correct settings are not adjusted, the screws will look like they are inserted properly, when the assembly is reopened later, the screws are oversized and show multiple mating errors. It was found that using a setting in the SolidWorks toolbox that mates the size of the screw with the size of the hole it is being placed in would fix this issue.

After handling these issues, we reviewed the CubeSat assembly, compared the finalized results to the P-POD requirements, and created our finalized CubeSat assembly. This assembly can be seen in Figure 16. After this design was solidified, it was used to run structural analysis. A final list of components is shown in Table 4.

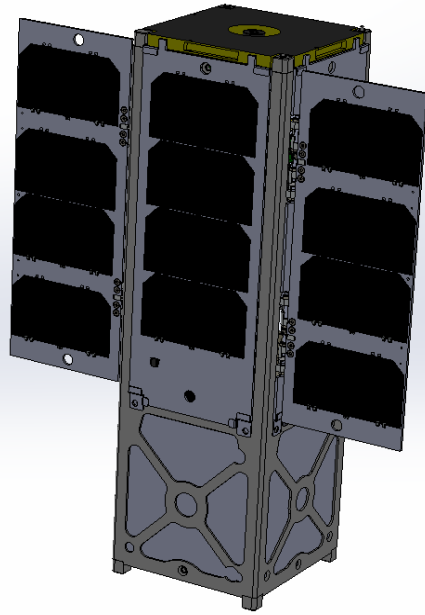


Figure 16: Completed CubeSat Assembly

Table 4: List of SphinX-NG CubeSat Components

Part	Quantity	Manufacturer
3U CubeSat Structure	1	Pumpkin, Inc.
SphinX-NG	1	Polish Academy of Sciences
2U Body Solar Panel	1	ClydeSpace
2U Deployable Solar Panel	2	ClydeSpace
UHF Antenna	1	ISIS
MT0.5-1 Magnetic Torquers	3	ZARM
Fine Sun Sensor	1	NewSpace Systems
CSS-01,02 Coarse Sun Sensor	4	Space Micro
SGR-05U GPS Receiver	1	Surrey Space Systems
ADXRS453 Gyroscope	1	Analog Devices
HMC5883L Magnetometer	1	Honeywell
Circuit Stack Mount	1	Custom
CubeSat OBC	1	ClydeSpace
USM-1192 Battery	1	ClydeSpace
USM-1335 EPS Board	1	ClydeSpace
TRXUV Transceiver	1	ClydeSpace
ADCS Board	1	
Solar Panel Clips (Top)	4	Pumpkin, Inc.
Solar Panel Clips (Bottom)	6	Custom

4 Structural Analysis

In this chapter, structural analysis is presented using the mechanical design outlined in Chapter 3. The structural analysis was performed using ANSYS in order to determine whether the completed SphinX-NG CubeSat assembly would be able to survive the vibration environment at launch and be compliant with P-POD requirements.

4.1 Review of Structural Analysis

The CubeSat design specification states that random vibration testing must be performed in accordance with the launch provider (Pignatelli, 2013). If the launch environment is unknown, the NASA Goddard Environmental Verification Standard can be used to derive testing requirements. Since the launch vehicle model for this mission is currently unknown, the GEVS requirements were used to conduct random vibration analysis. GEVS states that in the absence of knowledge of expected vibrations, the levels shown in Table 5 should be used.

Table 5: Random Vibration loads (Goddard Space Flight Center, 2013)

Frequency (Hz)	ASD Level (g^2/Hz)	
	Qualification	Acceptance
20	0.026	0.013
20-50	+6 dB/oct	+6 dB/oct
50-800	0.16	0.08
800-2000	-6 dB/oct	-6 dB/oct
2000	0.026	0.013
Overall	14.1 G_{rms}	10.0 G_{rms}

The qualification levels (14.1 G_{rms}) were used in order to ensure that the structural analysis covered all possible ranges of launch vehicle vibration.

In Billings et al. (2013), structural analysis using SolidWorks Simulation was performed. This analysis used the minimum workmanship levels provided by GEVS, which represent a 6.8 G_{rms}

vibration. However, these requirements are a minimum requirement and are primarily intended for electronic and electromechanical components (GSFC, 2013). Therefore, in this MQP we used the higher qualification vibration levels shown in Table 5 for our analysis.

Additionally, Billings et al. (2013) conducted vibration analysis on the structure itself. However, the masses of internal components inside the structure greatly affect how it responds to vibration loading, so we extended the simulation to include the internal components as well. Initial simulations on the structure were performed in SolidWorks in an attempt to validate the results of Billings et al. (2013). Through this analysis, similar results to Billings et al. (2013) were obtained. However, SolidWorks proved to be inadequate for the full-scale structural analysis including internal components, so ANSYS was used for the remainder of the analysis. ANSYS includes modules for modal and random vibration analysis, and provides greater control over the simulation.

4.2 Defeatured SphinX-NG CubeSat Model

In order for the ANSYS simulation to be able to run in a reasonable amount of time, a defeatured model of the SphinX-NG CubeSat assembly was created. The simplified structure from Billings et al. (2013) was used. Defeatured models of the solar panels, SphinX-NG, GPS receiver, antenna, stack, and magnetorquers were created using SolidWorks. Since the SphinX-NG CubeSat will be stowed inside the P-POD for the duration of the launch, the solar panels were modeled in their non-deployed configuration. The assembly model was then exported to a format compatible with ANSYS and is shown in Figure 17.

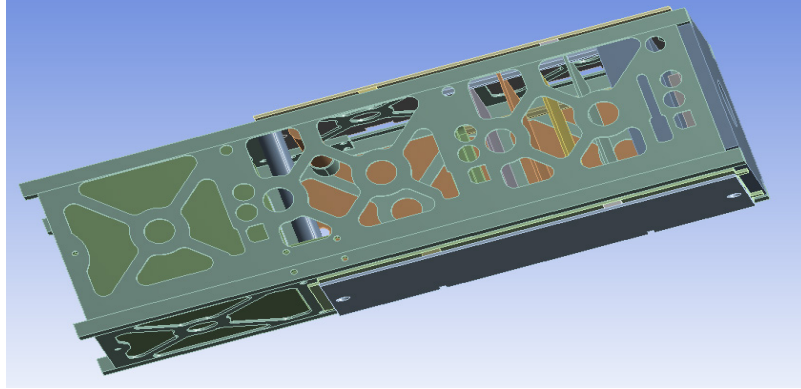


Figure 17: Simplified CAD Model in ANSYS

4.3 Analysis Setup in ANSYS

Random vibration analysis in ANSYS is based on the mode-superposition method (SHARCNet, 2015). Therefore, a modal study must first be performed in order to obtain the natural frequencies and mode shapes of the structure. A modal study was inserted into the ANSYS project as a base, and then three Random Vibration studies were inserted (one for each axis of vibration) to inherit data from the modal study.

The goal of the analysis was to determine the response of the structure under random vibration, so only stresses and deformations in the structure were of interest. The actual response of internal components was not of interest, as this would be determined by the component manufacturers. Therefore, internal components could be treated as rigid bodies for the analysis, while the structure was modeled as flexible in order to determine the stress and deformation. ANSYS allows designation of separate bodies within in assembly as flexible or rigid, so the structure was set as a flexible body while the other components were set as rigid.

With flexible/rigid bodies defined, contacts could be set up in the assembly to model how internal components are connected to the structure. For components mounted to the structure by

screws, a fixed joint connection was used. This type of connection prevents the screw hole on the structure from moving with respect to the screw hole in the component, which is a good approximation of a stiff screw. This type of contact was used for the SphinX-NG, magnetorquers, stack, and GPS. Due to the difficulty of modeling the clips used to hold on the solar panels, the solar panels were set as a bonded contact with the structure. The antenna was also modeled this way.

Setup for the modal analysis required defining boundary conditions and setting limits on the number and frequency of modes to find. For the boundary conditions, the “feet” of the structure were modeled as fixed to simulate confinement within the P-POD container (McBride, 2014). Since the GEVS standard gives a range of 20 – 2000 Hz for the loads, the modal analysis was limited to a range of 20 – 3000 Hz. This limit was set because 1.5x the maximum expected vibration frequency represents a good upper limit for the purposes of conducting a random vibration analysis in ANSYS (SHARCNet, 2015). The maximum number of modes to find was set to 100 because it was found that setting this value lower may prevent higher frequency modes from being found.

With the modal study complete, the random vibration studies could be performed. To set up the random vibration study, an acceleration spectral density (ASD) load was applied to the fixed boundary conditions. The ASD levels were set to the levels provided by GEVS. In order to improve computation time, the mode significance level was set to 1×10^{-4} in the analysis settings. This excludes insignificant modes from the analysis (SHARCNet, 2015).

4.4 Full-Scale Analysis Results

The modal analysis produced a list of modes and their corresponding frequencies as shown in

Figure 18. A total of 33 modes were found ranging from about 400 Hz to 2,940 Hz. With the lowest mode well above 100 Hz, there is no concern of the CubeSat having natural frequencies that resonate with the major launch vehicle forcing frequencies.

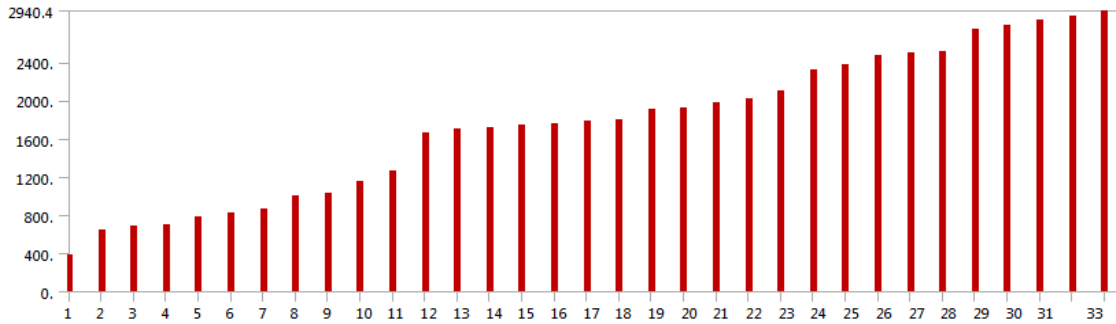


Figure 18: SphinX-NG CubeSat Modes

For the X-axis vibration, maximum stress was found to be concentrated around the SphinX mounting holes, and maximum deformation was located on the anti-sun side of the part of the structure containing the SphinX. The stress and deformation for the X-axis vibration are shown in Figure 19 and Figure 20.

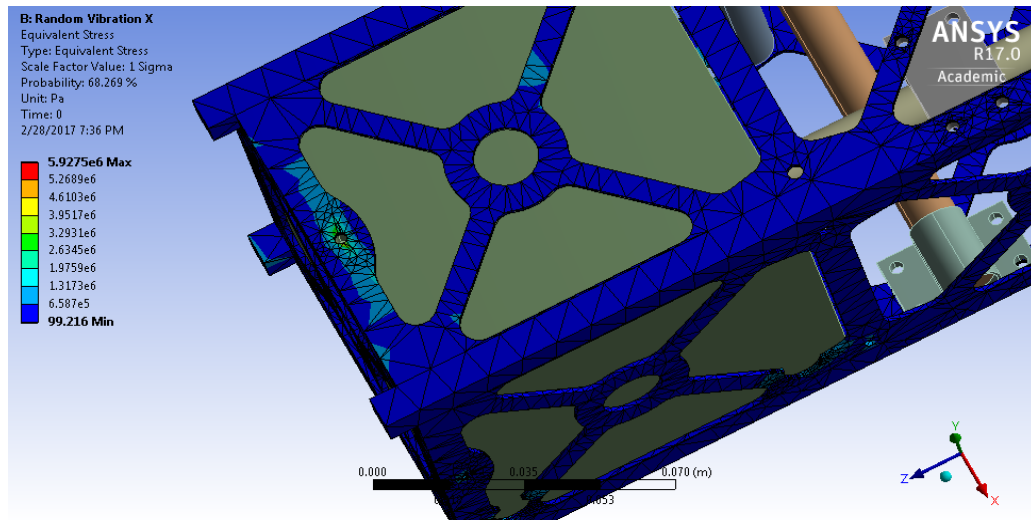


Figure 19: von Mises Stress (X-Axis Vibration)

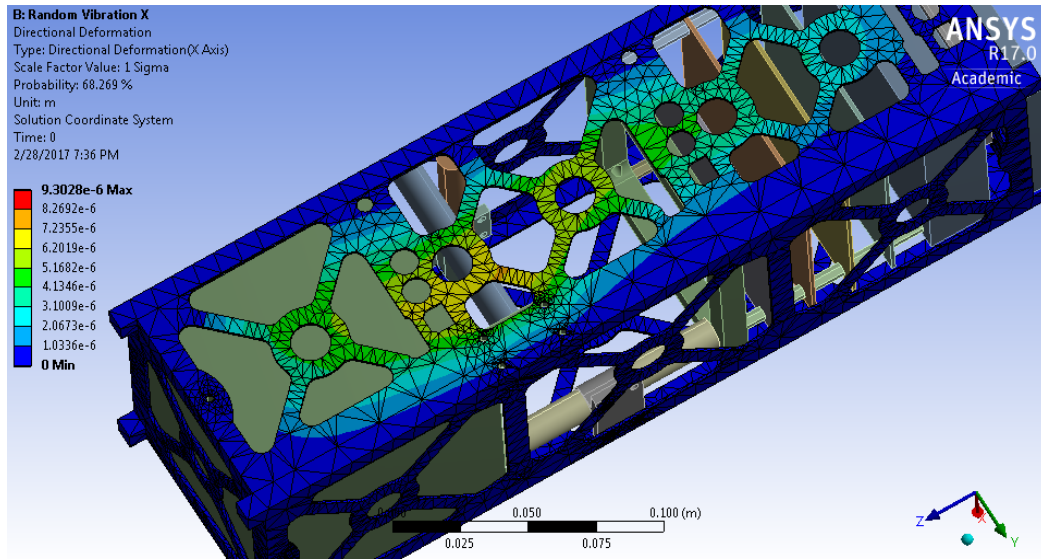


Figure 20: Deformation (X-Axis Vibration)

For the Y-axis vibration, maximum stress was once again found to be concentrated around the mounting holes for the X-axis magnetic torquer. Maximum deformation was located on the sun-facing side of the unit containing the SphinX. The stresses and deformations are shown in Figure 21 and Figure 22.

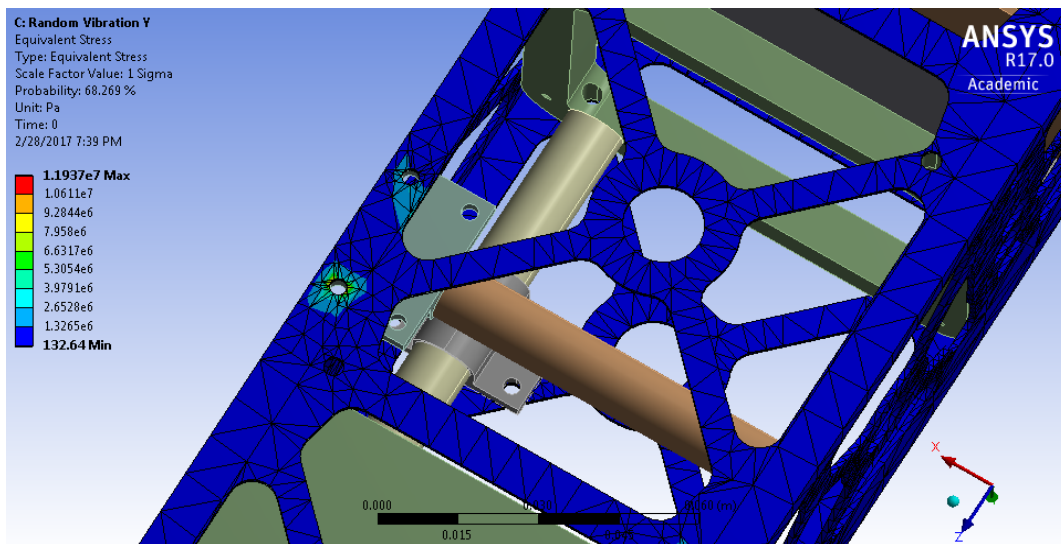


Figure 21: von Mises Stress (Y-Axis Vibration)

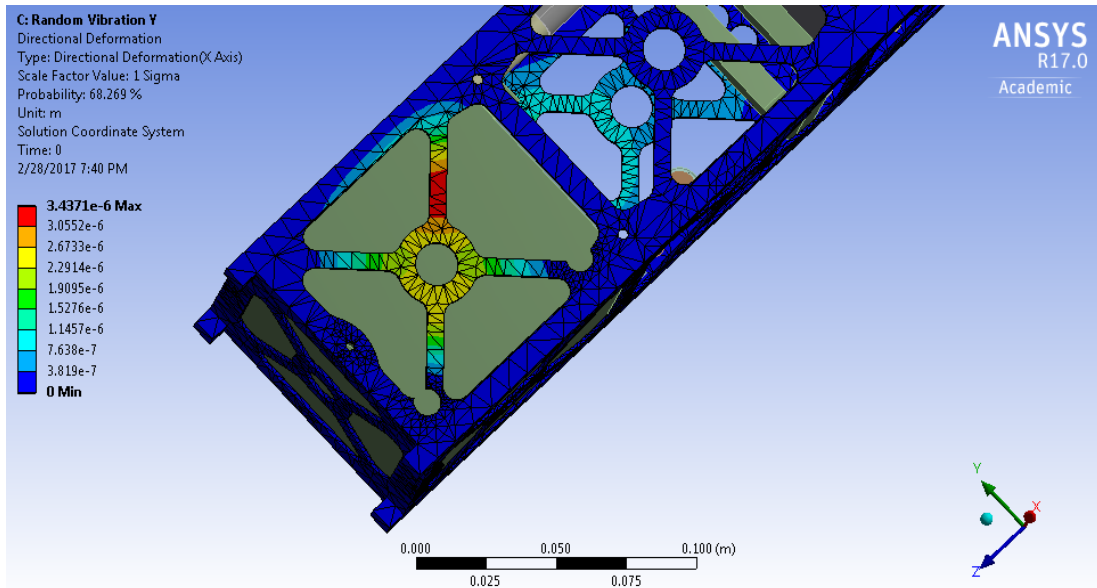


Figure 22: Deformation (Y-Axis Vibration)

For Z-axis vibration, the maximum stresses were within the unit containing the SphinX-NG as seen in Figure 23. Maximum deformation was located on the anti-sun-facing side of the SphinX-containing unit as shown in Figure 24.

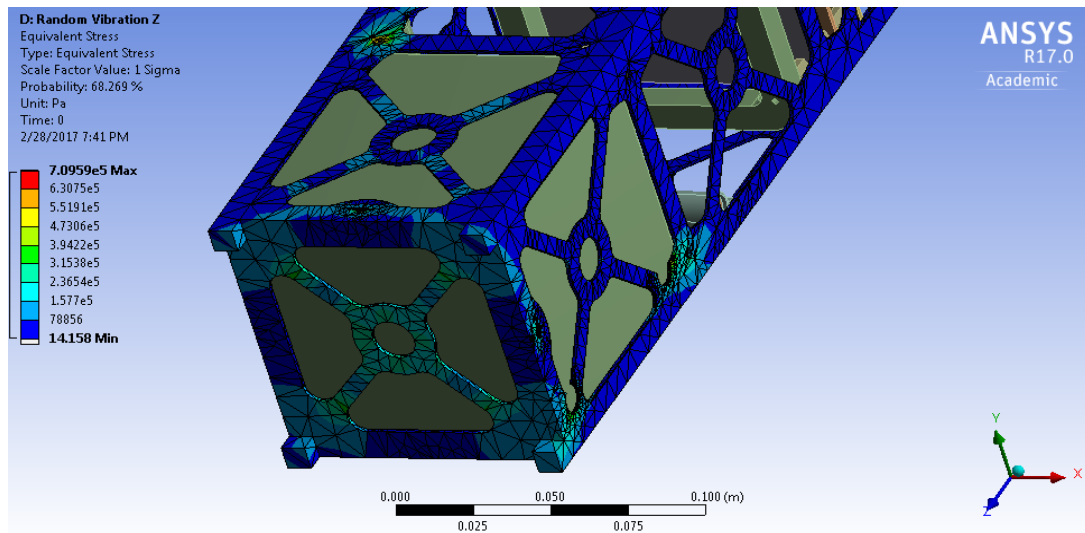


Figure 23: von Mises Stress (Z-Axis Vibration)

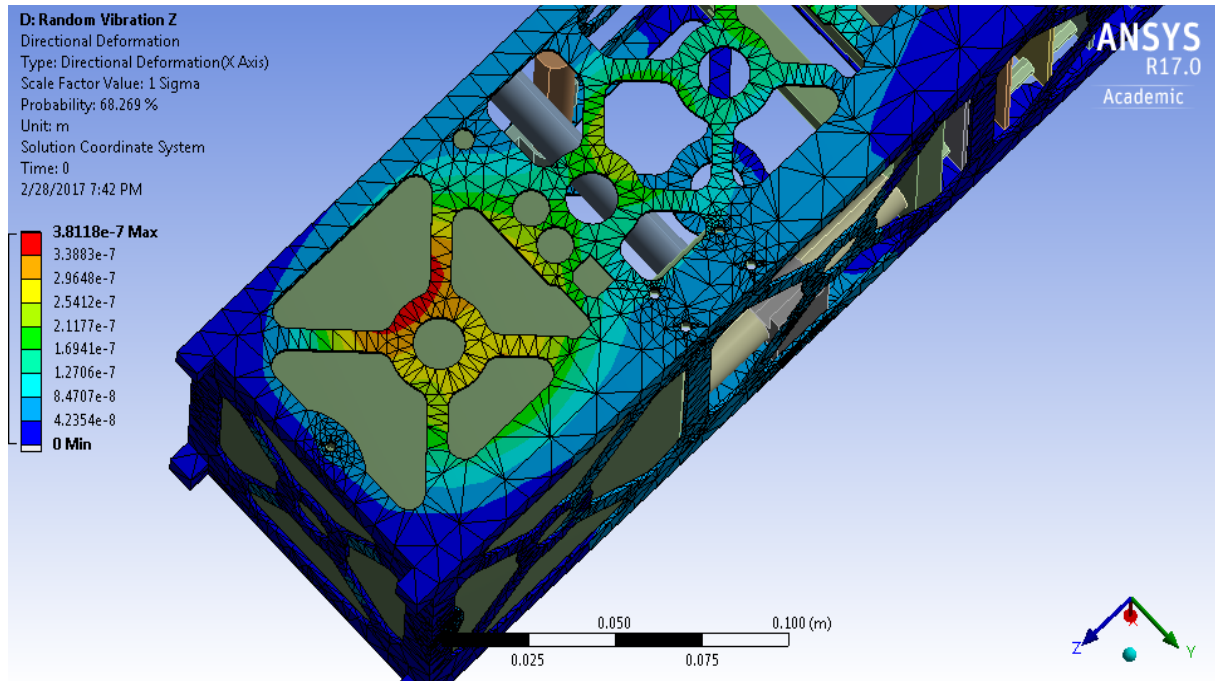


Figure 24: Deformation (Z-Axis Vibration)

Table 6 summarizes the maximum stress and deformation for each vibrational case.

Table 6: Maximum Stress and Deformation

Vibration Axis	Maximum Stress (MPa)	Maximum Deformation (m)
X	5.927	9.3028×10^{-6}
Y	11.937	3.4371×10^{-6}
Z	0.710	3.8118×10^{-6}
Overall	11.937	9.3028×10^{-6}

Note that the yield stress of the aluminum 5052-H32 used for the structure is 193 MPa (MatWeb). Therefore, the maximum stress is only 6.2% of the yield stress, representing a factor of safety of 16.2 against yielding. Additionally, the maximum deformation is approximately 10^{-5} m, which is too small to be a cause for concern.

4.5 Structural Analysis of Circuit Stack

In the full-scale structural analysis presented above, the circuit stack was treated as a rigid object in order to simplify the analysis. However, the circuit stack contains custom components such as the mounting bracket and standoffs. A separate structural analysis was conducted on the simplified stack assembly (shown in Figure 25), now treating these components as flexible bodies rather than rigid objects. Setup was performed in the same manner as before. In the modal analysis, the screw holes of the mounting plate were treated as the fixed support. Then, the GEVS profile was applied along each of the axes for the random vibration study.

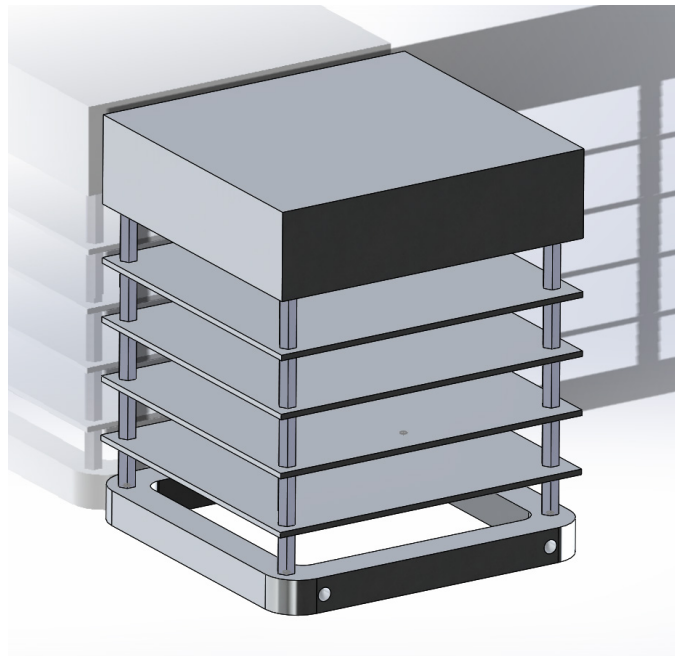


Figure 25: Simplified Stack CAD Model

The modal study found six modes ranging from 385 Hz to 2170 Hz as shown in Figure 26. Again, the lowest mode is well above the 100 Hz minimum required for launch vehicle compatibility.

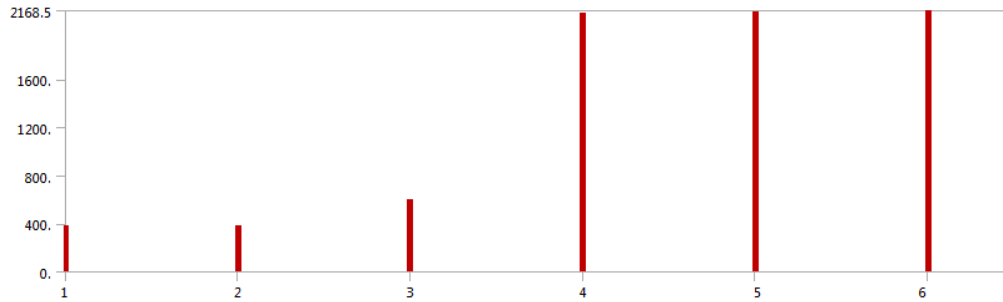


Figure 26: Stack Modes

Maximum stresses shown in Figure 27 are located on the threaded portion of the standoffs (where the cross-sectional area was minimum). Stress in the circuit boards was not evaluated, as these components should be manufacturer-tested.

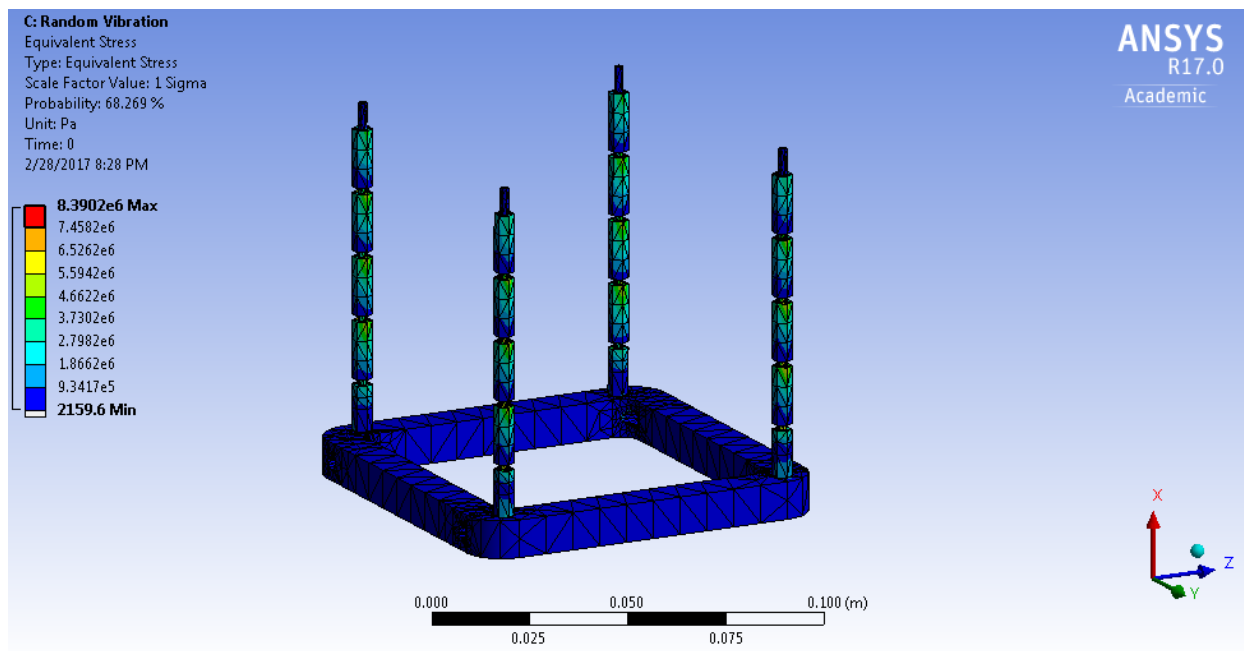


Figure 27: Worst Case von Mises Stress

The deformations of the circuit standoffs are shown in Figure 28. As expected, maximum deformation was located at the free ends of the standoffs. The maximum stress and deformation

occur when the random vibration is applied perpendicular to the standoff axial direction (when vibration is along the X and Y axes of the CubeSat coordinate system).

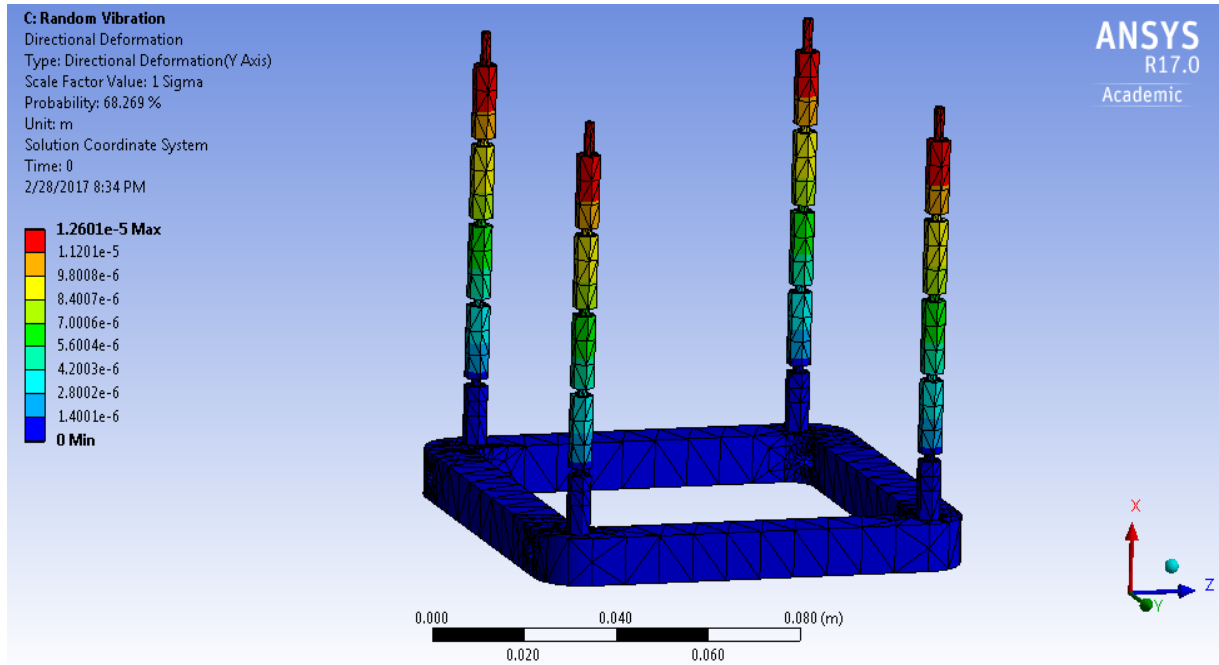


Figure 28: Worst Case Deformation

Table 7 summarizes the worst-case stress and deformation of the circuit stack.

Table 7: Maximum Stress and Deformation (Stack)

Maximum Stress (MPa)	Maximum Deformation (m)
8.39	1.260×10^{-5}

Note that the yield stress of the aluminum 6061-T6 used for the mounting plate and standoffs is 276 MPa (MatWeb). Therefore, the maximum stress is only 3.0% of the yield stress, representing a factor of safety of 32.9 against yielding. Additionally, the maximum deformation is on the order of 10^{-5} m, which is not large enough to be a cause for concern.

5 Analysis of Electromagnetic Interference

The CubeSat uses a magnetometer to measure the strength of Earth's magnetic field and determine its orientation. Magnetic torquers are used on the SphinX-NG CubeSat for attitude control (MAD-1701). If the magnetic field induced by the magnetic torquers is significant at the location of the magnetometer, it could interfere with the magnetometer readings, causing the CubeSat to lose track of its orientation. Analysis of the magnetic fields produced by the magnetic torquers was conducted using the AC/DC module in the COMSOL software package.

5.1 Review of Electromagnetic Interference Analysis

Billings et al. (2013) conducted an analysis including all three magnetic torquers inside of an aluminum rectangular prism representing the SphinX-NG CubeSat structure. They predicted a maximum B field of 1167.88 G and a minimum field of 8.375×10^{-8} G at the outer edge of the analysis domain when all three magnetic torquers were active. The aluminum prism completely enclosed the magnetic torquers, whereas the actual structure has numerous gaps and holes exposing the internals to free space. In this chapter, the COMSOL simulation was updated to use the simplified structure used for structural analysis, thus accounting for the gaps in the structure.

5.2 Analytical Solution of a Solenoid

An analytical solution of a single solenoid was obtained in order to validate the results obtained through COMSOL. The magnetic moment of a current loop is given by the following, where the variables are as in Table 8:

$$\mu = nIA \quad (1)$$

Table 8: Magnetic Torquer Parameters

Variable	Meaning	Units	Value
μ	Magnetic moment	A*m ²	0.5
n	Number of turns	None	Unknown
I	Coil current	A	0.06
A	Coil area	m ²	1.120*10 ⁻⁴
r	Radius of magnetorquer	m	0.00597
l	Length of magnetorquer	m	0.09398

Solving for n gives 73,683 turns in each magnetic torquer. The surface current K_0 of the coil is given by the following:

$$K_0 = \frac{nI}{l} \quad (2)$$

This yields a surface current of 47,515.6 A/m. The surface current will be used as an input for the COMSOL simulation.

The magnetic flux density produced by a solenoid aligned with the Z-axis is given by:

$$B = \frac{\mu K_0}{2} \left(\frac{\frac{l}{2r} - \frac{z}{r}}{\sqrt{1 + \left(\frac{l}{2r} - \frac{z}{r}\right)^2}} + \frac{\frac{l}{2r} + \frac{z}{r}}{\sqrt{1 + \left(\frac{l}{2r} + \frac{z}{r}\right)^2}} \right) \quad (3)$$

Where all parameters are as defined in Table 8, but μ is now the permittivity of free space ($\mu = 4\pi*10^{-7}$ H/m), and z is the z-coordinate along the solenoid (with $z = 0$ at the center). This produces a magnetic field of 592.3 G at the center and 297.9 G at the ends.

5.3 COMSOL Modeling of a Single Magnetic Torquer

A model of a single magnetic torquer was created in COMSOL to check the numerical results against the analytical solution performed in Section 5.2. The model was a single cylinder with the dimensions in Table 8 and the surface current calculated in Section 5.2. Probes were inserted at the center and the end of the cylinder, and the results are summarized in Table 9. A multi-slice plot of the normal magnetic flux density is shown in Figure 29.

Table 9: Comparison of Analytical and COMSOL B Field Intensity for a Single Magnetic Torquer

Location	Analytical B Field (G)	COMSOL B Field (G)	% Difference
Center	592.3	592.0	0.05
Ends	297.9	297.6	0.11

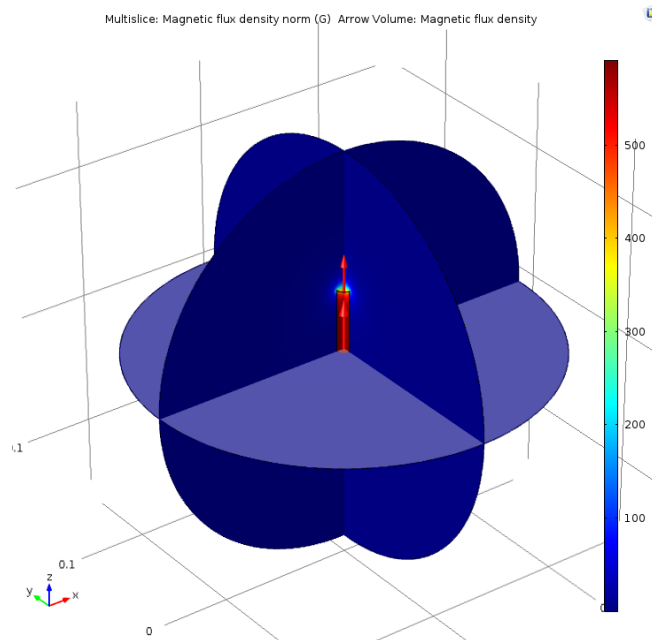


Figure 29: Multi-Slice Plot of a Single Magnetic Torquer

The results obtained by COMSOL are very accurate, so it is safe to extend the COMSOL model to include multiple magnetic torquers.

5.4 COMSOL Modeling of Multiple Magnetic Torquers

In order to create a COMSOL model of the magnetic torquers, a simplified SolidWorks assembly containing the structure, stack, and the magnetic torquers was first created. This assembly (shown in Figure 30) was imported into COMSOL, and the AC/DC module was used to set up a magnetic field study.

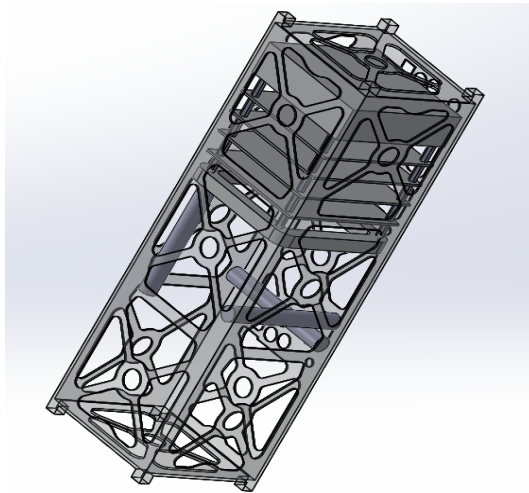


Figure 30: CAD Model used for COMSOL Simulation

Three surface currents were inserted into the study, one for each magnetic torquer. The surface current calculated in Section 5.2 was used as an input. Additionally, a sphere was inserted to define the space over which the analysis would be conducted. A material assignment of Al-5052 H32 was made to the structure, and Al-6061 T6 to the structural components of the stack. Aluminum has a relative permeability of 1, and therefore the structure is not expected to greatly affect the induced magnetic fields. Due to the complexity of the printed circuit boards in the stack, the permeability of the stack components is unknown and was not considered in this simulation.

5.5 Discussion of Results

The maximum magnetic flux density was found to be 1176 G near the magnetic torquers. However, the magnetic flux density decreases rapidly with distance from the centers of the magnetorquers. A probe at the location of the magnetometer, predicted that the magnetic flux density is 0.15 G. The magnetic flux density on planes intersecting at the magnetometer location is shown in Figure 31. Areas shown in red exceed the 8 G range of the magnetometer. Additionally, the magnetic field streamlines are shown in Figure 32.

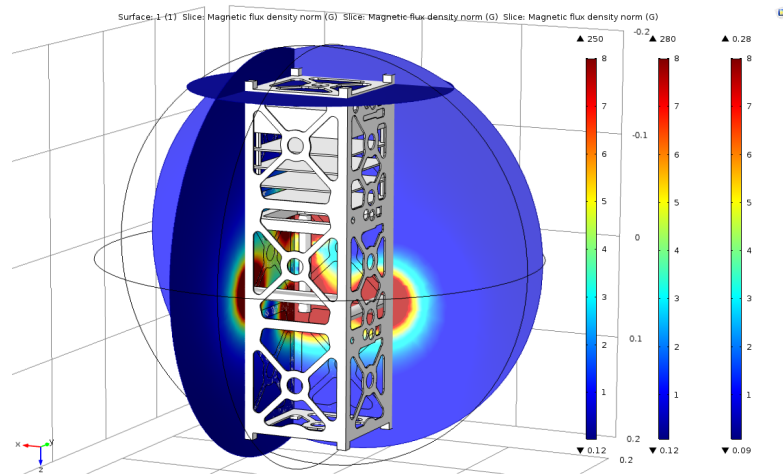


Figure 31: Magnetic Flux Density on Planes Intersecting at Magnetometer Location

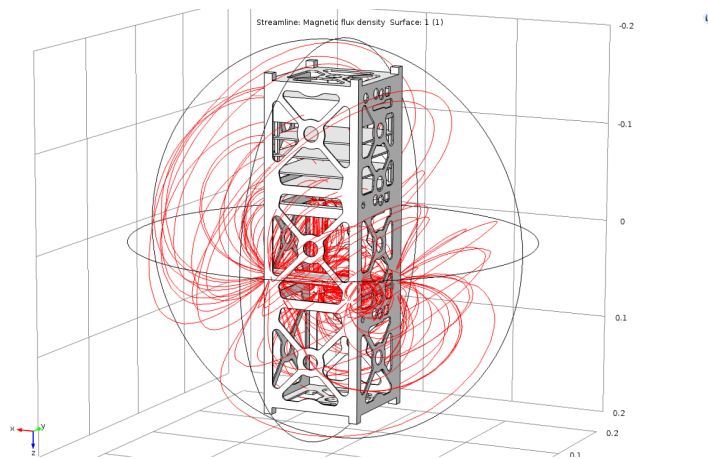


Figure 32: Magnetic Field Streamlines

The Earth's magnetic field at the SphinX-NG altitudes are 0.25 to 0.65 G (NOAA). The magnetometer selected by the MAD-1701 team has a range of -8 to 8 G, so the magnetic flux density observed at the magnetometer location will not exceed the allowable range. However, the magnetic flux density observed is on the order of the ambient magnetic flux density and will cause interference with the magnetometer readings.

Several options exist to counter the problem of electromagnetic interference. The Dopart et al. (2012) team suggested the use of a magnetometer boom to locate the magnetometer further away from the magnetic torquers. However, this option adds a great deal of complexity to the CubeSat design. Since the B field will not exceed the -8 to 8 G range of the magnetometer and the induced B field is known at the magnetometer location, the ADC software could be modified to subtract the value of the induced field from the magnetometer reading before using the data in the control algorithm. Another option is to use magnetic insulating material between the magnetorquers and the magnetometer. This would reduce the induced magnetic field at the magnetometer location, but the shielding material could also interfere with the ambient magnetic field and prevent the CubeSat from obtaining its orientation. An additional option is to only take magnetometer readings when the magnetorquers are off, so that there is no induced field to interfere with the readings.

6 Conclusions and Recommendations

This MQP is part of a larger conceptual design of a 3U CubeSat, which carries the Solar Photometer in X-rays-Next Generation (SphinX-NG) instrument. The overall goal of the mission is to place the CubeSat into a polar, sun-synchronous orbit at an altitude of 450-650 km so the SphinX-NG can perform solar and extraterrestrial X-ray spectroscopy. A group of 12 aerospace engineering majors constituted the Systems Engineering Group (SEG). The SEG was split into three separate teams (and MQPs) addressing the various subsystems and mission operations of the SphinX-NG CubeSat:

- Orbital, Mechanical, Structural, and Environmental (NAG-1701)
- Power, Thermal, Command and Data, Communications, Mission Ops (JB3-1701)
- Attitude Determination and Control (MAD-1701)

The approaches and conclusions of this MQP are outlined below.

6.1 Orbital Analysis

The first objective of this MQP was to conduct orbital analysis to ensure the CubeSat could be launched to an appropriate orbit and meet deployer requirements. The P-POD deployer was selected due to its versatility in the range of achievable orbits. Orbital analysis was completed using the STK software, and lifetime analysis using the NRLMSISE-00 atmospheric model identified a 600 km polar orbit as the best option. The lifetime decay was 17.8 years, which fell well below the requirement of 25 years or less for orbital decay. The chosen orbit also allows the SphinX-NG instrument to complete its science objectives. The SphinX-NG CubeSat CAD file was integrated into STK, so other design teams could conduct detailed analysis.

6.2 Mechanical Design

The second objective of this MQP was to complete the mechanical design to ensure full compliance with the P-POD deployer requirements. The CAD files from Billing et al. (2013) were used as a starting point and updated with new instruments and sensors from the other MQP design teams. The final design was reconfigured to keep the center of mass within 2 cm of the geometric center and includes a defeatured SphinX-NG instrument occupying the 1U of the structure.

6.3 Structural Analysis

The third objective of this MQP was to conduct structural analysis on the completed CAD design to determine if the CubeSat could withstand the launch environment. Using SolidWorks, a defeatured model of the SphinX-NG CubeSat was created. Modal and random vibration analysis was conducted using ANSYS. The resulting stresses and deformations of the structure were well within acceptable limits, indicating that the SphinX-NG CubeSat will be able to survive the worst-case launch environment.

6.4 Environmental Analysis

The final objective of this MQP was to conduct environmental analysis to determine if the magnetic fields produced by the magnetic torquers would interfere with the magnetometer readings. A comparison between the analytical and numerical COMSOL solution for a single torquer was used for validation. Using COMSOL, a model of the magnetic field produced from the all three magnetorquers was developed. The structure and circuit stack were included in the analysis. Analysis showed the magnetic field produced is on the same order of magnitude as the ambient field. Several options to address this issue are discussed in sections 5.5 and 6.5.

6.5 Recommendations

Overall this MQP met all the objectives. Several recommendations for future work are outlined below.

- Acquire a final design of the SphinX-NG instrument from the Space Research Center (SRC) at the Polish Academy of Sciences. The design should conform to P-POD requirements. Once the design is completed, future teams should integrate the new CAD model in the CubeSat assembly and run the mass analysis again to determine if the center of mass is still located within a 2 cm sphere of the geometric center.
- Perform structural analysis to use more accurate methods for determining the effects of the solar panel mounting clips. In reality, the solar panels are free to move with respect to the structure, but are constrained by the clips. In the structural analysis, the solar panels were bonded to the structure itself. It is recommended that future teams look into methods to better model the real behavior of the clips.
- Identify ways to reduce the influence of the magnetic field created by the magnetorquers on the magnetometer. Several options are available to address this concern. One option is to add shielding between the magnetorquers and the magnetometer. Another option is to attach the magnetometer to a boom so it can extend past the influence of the induced magnetic field. A third option is to subtract the (known) induced field from the magnetometer readings in the ADC software. The last option would require the magnetometer to only be used when the magnetorquers are off. Additionally, the effects of the stack circuit boards and battery on induced fields should be researched.

References

- Billings, D., Graedel, I., Hoey, F., Lavallee, P., Martinez, N., & Torres, J. (2013, Feb. 25). *Design and Analysis for a CubeSat Mission* (NAG-1204). Worcester Polytechnic Institute, Worcester, MA.
- CubeSat concept - eoPortal Directory - Satellite Missions. 2017. *CubeSat concept - eoPortal Directory - Satellite Missions*. [online] Available at: <https://directory.eoportal.org/web/eoportal/satellite-missions/c-missions/cubesat-concept>. [Accessed 17 March 2017].
- Davis, J. (2012, Apr. 11). *Of inclinations and azimuths*. [online] Available at: <http://www.planetary.org/blogs/guest-blogs/jason-davis/3450.html>. [Accessed 17 March 2017].
- Dopart, C., Morlath, R., Oliver, E., & Schomaker, J., (2012, Mar. 1). *Design and Analysis for a CubeSat Mission* (NAG-1102). Worcester Polytechnic Institute, Worcester, MA.
- Globalcom. 2006. *The Cost of Building and Launching a Satellite*. [online] Available at: <http://www.globalcomsatphone.com/hughesnet/satellite/costs.html>. [Accessed 17 March 2017].
- Greby, M. (2015, July 2). *Pacific Spaceport Complex - Alaska Range User's Manual*. [online] Available at: <http://akaerospace.com/sites/default/files/download/PSCA%20RUM%20July%202015%20R1.pdf> [Accessed 17 March 2017].
- Heyman, Jos. 2009. *FOCUS: CubeSats — A Costing + Pricing Challenge*. [online] Available at: <http://www.satmagazine.com/story.php?number=602922274>. [Accessed 17 March 2017].
- Jacchia, L.G. (1964). “Static Diffusion Models of the Upper Atmosphere with Empirical Temperature Profiles.” *Smithsonian Contributions to Astrophysics*, [online]. 8, 215. Available at: <http://articles.adsabs.harvard.edu//full/1965SCoA....8..215J/0000215.000.html>. [Accessed 17 March 2017].
- Kulu, Erik. 2017. *Nanosatellite & CubeSat Database | NewSpace Constellations, Nanosat Companies, CubeSat Technologies and Instruments*. [online] Available at: <http://www.nanosats.eu/>. [Accessed 17 March 2017].
- MatWeb, LLC. *Aluminum 5052-H32*. [online] Available at: <http://www.matweb.com/search/datasheet.aspx?matguid=96d768abc51e4157a1b8f95856c49>

- [028](#). [Accessed 17 March 2017].
- MatWeb, LLC. *Aluminum 6061-T6; 6061-651*. [online] Available at:
<http://www.matweb.com/search/DataSheet.aspx?MatGUID=b8d536e0b9b54bd7b69e4124d8f1d20a>
- McBride, R. (2014, Mar. 31). *ANSYS – Modal Analysis of a Satellite*. [online] Available at:
<https://confluence.cornell.edu/display/SIMULATION/ANSYS+-+Modal+Analysis+of+a+Satellite> [Accessed 17 March 2017].
- NASA Goddard Space Flight Center. (2013, Apr. 22). *General Environmental Verification Standard (GEVS)* (GFSC-STD-7000A). [online] Available at:
<https://standards.nasa.gov/standard/gsfsc/gsfsc-std-7000> [Accessed 17 March 2017].
- NASA Lyndon B. Johnson Space Center. (January, 2012). *Debris Assessment Software User's Guide*. Retrieved on September 27, 2016 from
https://orbitaldebris.jsc.nasa.gov/library/das2_0_2/das2.0_usersguide.pdf
- National Aeronautics and Space Administration (October, 1976). U.S. Standard Atmosphere, 1976. [online] Available at: <http://ntrs.nasa.gov/archive/nasa/casi.ntrs.nasa.gov/19770009539.pdf> [Accessed 17 March 2017].
- National Oceanic and Atmospheric Administration (NOAA). *Geomagnetism Frequently Asked Questions*. [online] Available at: <https://www.ngdc.noaa.gov/geomag/faqgeom.shtml> [Accessed 17 March 2017].
- Oliva, A., Schaalman, G., Staley, S., (Mar. 15, 2011). *Design and Analysis for a CubeSat Mission* (NAG-1002). Worcester Polytechnic Institute, Worcester, MA.
- Petty, J. National Aeronautics and Space Administration. (2002, Apr. 7). *Launch Sites*. [online] Available at: <https://spaceflight.nasa.gov/shuttle/reference/shutref/sts/launch.html> [Accessed 17 March 2017].
- Picone, J.M. (2001, Dec.). Laboratory for Atmospheres NASA Goddard Space Flight Center. *NRLMSISE-00 Empirical Model of the Atmosphere: Statistical Comparisons and Scientific Issues*. [online] Available at:
<https://ntrs.nasa.gov/archive/nasa/casi.ntrs.nasa.gov/20020038771.pdf> [Accessed 17 March 2017].
- Pignatelli, DP, 2013. CubeSat Design Specifications. *The CubeSat Program, Cal Poly SLO*, [online]. 13, 1-42. Available

- at: https://static1.squarespace.com/static/5418c831e4b0fa4ecac1bacd/t/56e9b62337013b6c063a655a/1458157095454/cds_rev13_final2.pdf [Accessed 17 March 2017].
- Planet. 2017. *Planet — Approach*. [online] Available at: <https://www.planet.com/company/approach/>. [Accessed 17 March 2017].
- QuakeFinder - About QuakeSat. (n.d.). [online] Available at: <https://www.quakefinder.com/science/about-quake-sat/> [Accessed 17 March 2017].
- SHARCNet. (2015, Dec. 02). *Random Vibration Analysis*. [online] Available at: https://www.sharcnet.ca/Software/Ansys/17.0/en-us/help/wb_sim/ds_spectral_analysis_type.html [Accessed 17 March 2017].
- Swartwout, M. (2016, August 31). CubeSat Database. [online] Available at: <https://sites.google.com/a/slu.edu/swartwout/home/cubesat-database> [Accessed 17 March 2017].
- Sylwester, J., M. Kowalinski¹, S. Gburek¹, M. Siarkowski¹, S. Kuzin², F. Farnik³, F. Reale⁴, K. J. H. Phillips⁵, J. Baka La¹, M. Gryciuk¹, P. Podgorski¹, B. Sylwester, SphinX Measurements of the 2009 Solar Minimum X-Ray Emission, *Astrophysical Journal*, 2012. [online] Available at: <http://arxiv.org/pdf/1203.6809.pdf> [Accessed 17 March 2017].
- Sylwester, L., S. Kuzin, Yu. D. Kotov, F. Farnik, F. Reale, SphinX: A fast solar Photometer in X-rays, *Journal of Astrophysics and Astronomy*, 2008. [online] Available at: <https://link.springer.com/article/10.1007/s12036-008-0044-8> [Accessed 17 March 2017].
- Systems Tool Kit. 2017. *Orbit Propagators for Satellites*. [online] Available at: http://help.agi.com/stk/index.htm#stk/vehSat_orbitProp_choose.htm. [Accessed 17 March 2017].
- Waite, A. (n.d.). *Kodiak Launch Complex (KLC) -aka- Alaska Orbital Launch Complex (AOLC) History and lessons*. [online] Available at: <http://www.spaceops2012.org/proceedings/documents/id1295313-Paper-002.pdf> [Accessed 17 March 2017].

Appendix A: List of P-POD Requirements

CubeSat Specification			
General Requirements			
Requirement	Our Cubesat	Group Responsible	Compliance
Any deviation from the CDS shall submit a DAR and adhere to the wavier process	N/A	N/A	N/A
All parts shall remain attached to the CubeSats during launch, ejection and operation. No additional space debris shall be created.		Structures	
Pyrotechnics shall not be permitted.	None on CubeSat	All	Yes
No pressure vessels over 1.2 std atmosphere shall be permitted.	N/A	N/A	N/A
Pressure vessels shall have a factor of safety no less than 4.	N/A	N/A	N/A
Total stored chemical energy shall not exceed 100 Watt-Hours.	Carries a 30 Watt-Hour battery	Power	Yes
No hazardous materials shall be used on a CubeSat.	None on CubeSat	All	Yes
CubeSat materials shall satisfy the following low out-gassing criterion to prevent contamination of other spacecraft during integration, testing, and launch.		Structures	
Total Mass Loss shall be less than or equal to 1%	No Mass Loss	Structures	Yes
Collected Volatile Condensable Material shall be less than or equal to 0.1%	None on CubeSat	Structures	Yes
The latest revision of the CubeSat Design Specification shall be the official version	All revisions meet Design Specifications	Structures	Yes

Mechanical Requirement			
Requirement	Our Cubesat	Group Responsible	Compliance
The CubeSat shall use the coordinate system defined in Figure 5. The -Z face of the CubeSat will be inserted first into the P-Pod.	CubeSat uses the coordinate system so the Z axis goes down to the SphinX-NG, which is how it should be deployed from P-POD	Structures	Yes
The CubeSat configuration and physical dimensions shall be per Figure 5.	Yes, the CubeSat is within the dimensional limits	Structures	Yes
CubeSat shall be 100.0 +/- 0.1 mm wide	Yes, the CubeSat is within the dimensional limits	Structures	Yes
CubeSat shall be 340.5+/-0.3 mm tall	Yes, the CubeSat is within the dimensional limits	Structures	Yes
All components shall not exceed 6.5 mm normal to the surface of the P-POD, other than the designated CubeSat rails		Structures	
Deployables shall be constrained by the CubeSat. The P-POD rails and walls shall not be used to constrain deployables		Structures	
Rails shall have a minimum width of 8.5 mm		Structures	
The rails shall not have a surface roughness greater than 1.6 micro meters		Structures	
The edges of the rails shall be rounded to a radius of at least 1 mm		Structures	
The ends of the rails on the +Z face shall have a minimum surface area of 6.5 mm x 6.5 mm contact area for neighboring CubeSat rails		Structures	
At least 75% of the rails shall be in contact with the P-POD rails. 25% of the rails may be recessed and no part of the rails shall exceed the specification (at least 255.4 mm rail contact)		Structures	

Mass			
Requirement	Our Cubesat	Group Responsible	Compliance
CubeSat shall not exceed 4.0 kg mass		Structures	
The CubeSat center of gravity shall be located within a sphere of 2 cm from its geometric center		Structures	
Materials			
Requirement	Our Cubesat	Group Responsible	Compliance
Aluminum 7075 or 6061 shall be used for both the main CubeSat structure and the rails. If other materials are used the developer shall submit a DAR and adhere to the waiver process		Structures	
The CubeSat rails and standoff, which contact the P-Pod rails and adjacent CubeSat standoffs, shall be hard anodized aluminum to prevent and cold welding with the P-POD		Structures	

Electrical Requirements			
Requirement	Our Cubesat	Group Responsible	Compliance
No electronics shall be active during launch to prevent any electrical or RF interference with the launch vehicle and primary payload. CubeSats with batteries shall be fully deactivated during launch or launch with discharged batteries	Our CubeSat will launch fully deactivated	Power/CD&H	Yes
The CubeSat shall include at least one deployment switch on the designated rail standoff to completely turn off satellite power once actuated. In the actuated state, the deployment switch shall be centered at or below the level of standoff		CD&H	
All systems shall be turned off, including real time clocks		Power/CD&H	
To allow for CubeSat diagnostics and battery charging after the CubeSats have been integrated into the P-Pod all CubeSat umbilical connectors shall be within the designated Access Port location, green shaded areas shown in Figure 5		Power/CD&H	Yes
CubeSat deployment switch shall be depressed while inside the P-Pod. All diagnostics and battery charging shall be done while the deployment switch is depressed		Power/CD&H	Yes
The CubeSat shall include a Remove Before Flight pin or launched with batteries fully discharged. The pin shall be removed from the CubeSat after integration into the P-Pod		Power/CD&H	
3U Cubesats shall locate their pin in one of the 3 designated Access Port locations shown in Appendix C		Power/CD&H	
The pin shall cut all power to the satellite once it is inserted into the satellite		Power/CD&H	
The pin shall not protrude more than 6.5 mm from the rails when it is fully inserted into the satellite		Power/CD&H	

Operational Requirements			
Requirement	Our Cubesat	Group Responsible	Compliance
CubeSats with batteries shall have the capability to receive a transmitter shutdown command as per Federal Communications Commission regulation		Power/CD&H/Telecom	
All deployables such as booms, antennas, and solar panels shall wait to deploy a minimum of 30 minutes after the CubeSat's deployment switches are activated from P-POD ejection		CD&H	
RF transmitters greater than 1 mW shall wait to transmit a minimum of 30 minutes after the CubeSat's deployment switches are activated from P-POD ejection		CD&H/Telecomm	
Operators shall obtain and provide documentation of proper licenses for use of frequencies		Telecomm	
Orbital decay lifetime of the CubeSats shall be less than 25 years after end of mission life	At a 600 km orbit, the decay is below the 25 year limit	Orbital	Yes
Cal Poly shall conduct a minimum of one fit check in which developer hardware shall be inspected and integrated into the P-POD. A final fit check shall be conducted prior to launch. The CubeSat Acceptance Checklist shall be used to verify compliance of the specification		Orbital	

Testing			
Requirement	Our Cubesat	Group Responsible	Compliance
Random Vibration		Structures	
Subjected to Random Vibration Test to verify its ability to survive the lift-off environment and also to provide a final workmanship vibration test. For small payloads the test is required. The acoustic environment at lift-off is usually the primary source of random vibration, however other sources of random vibration must be considered. Protoflight hardware shall be subjected to a random vibration test to verify flightworthiness and workmanship. The test level shall represent the qualification level (flight limit level plus 3 dB). The test should cover the full 20-2000 Hz frequency range.		Structures	
Thermal Vacuum Bakeout		Thermal	
Commence with Bakeouts at the parts level, if possible. Bakeout hardware at the highest temperature possible.		Thermal	
Set quantitative acceptance criteria for each bakeout. These criteria should be based on the total allowable outgassing level for the spacecraft. Usually computer modeling analyses aid in the determination of the allowable outgassing level for hardware.		Thermal	
Do not accept hardware which does not meet the acceptance criteria or adjust the outgassing cleanliness budget accordingly.		Thermal	
As parts become assembled, often, the maximum temperature limits become lower. Bakeouts at lower temperatures are less effective, and take considerably longer to complete		Thermal	
Develop a detailed Thermal Vacuum Bakeout and Certification Plan for your program. Include the overall plan, schedule, need for instrumentation, and QCM acceptance criteria, as well as a list of the responsible individuals to contact during the test.		Thermal	
Visual Inspection		Structures	
Visual inspection of the CubeSat and measurement of critical areas shall be performed per the 3U CAC		Structures	